nature communications

Article

https://doi.org/10.1038/s41467-025-56309-8

Klebsiella pneumoniae employs a type VI secretion system to overcome microbiota-mediated colonization resistance

Received: 13 February 2024

Accepted: 15 January 2025

Published online: 22 January 2025

Check for updates

Andrew S. Bray[1], Christopher A. Broberg[2], Andrew W. Hudson[1], Weisheng Wu[3], Ravinder K. Nagpal[4], Md Maidul Islam[1], Juan D. Valencia-Bacca[1], Fawaz Shahid[5], Giovanna E. Hernandez[1], Noah A. Nutter[1], Kimberly A. Walker[2], Emma F. Bennett[1], Taylor M. Young[1], Andrew J. Barnes[1], David A. Ornelles[1], Virginia L. Miller[2,6] & M. Ammar Zafar[1,7]

Microbial species must compete for space and nutrients to persist in the gastrointestinal (GI) tract, and our understanding of the complex pathobiont-microbiota interactions is far from complete. *Klebsiella pneumoniae*, a problematic, often drug-resistant nosocomial pathogen, can colonize the GI tract asymptomatically, serving as an infection reservoir. To provide insight on how *K. pneumoniae* interacts with the resident gut microbiome, we conduct a transposon mutagenesis screen using a murine model of GI colonization with an intact microbiota. Among the genes identified were those encoding a type VI secretion system (T6SS), which mediates contact-dependent killing of gram-negative bacteria. From several approaches, we demonstrate that the T6SS is critical for *K. pneumoniae* gut colonization. Metagenomics and in vitro killing assays reveal that *K. pneumoniae* reduces *Betaproteobacteria* species in a T6SS-dependent manner, thus identifying specific species targeted by *K. pneumoniae*. We further show that T6SS gene expression is controlled by several transcriptional regulators and that expression only occurs in vitro under conditions that mimic the gut environment. By enabling *K. pneumoniae* to thrive in the gut, the T6SS indirectly contributes to the pathogenic potential of this organism. These observations advance our molecular understanding of how *K. pneumoniae* successfully colonizes the GI tract.

The microbiome of the gastrointestinal (GI) tract is a complex environment containing trillions of individual bacteria comprising hundreds of species[1] that are intrinsically linked to human health[2]. A critical role of the gut microbiome is to restrict the growth of incoming pathogens, a phenomenon known as colonization resistance (CR)[3–5] that involves microbial-mediated competition in addition to the host-provided immune defenses[2]. Epidemiological studies have demonstrated that inter-individual differences in microbiota composition can impact susceptibility to enteric infections[6,7]. Diet, immuno-suppressants, proton pump inhibitors, and antibiotics can influence the microbiota, resulting in reduced CR and increased susceptibility to pathogenic bacteria, such as multi-drug resistant *Klebsiella*

[1]Department of Microbiology and Immunology, Wake Forest School of Medicine, Winston Salem, NC, USA. [2]Department of Microbiology and Immunology, University of North Carolina School of Medicine, Chapel Hill, NC, USA. [3]BRCF Bioinformatics Core, University of Michigan, Ann Arbor, MI, USA. [4]Department of Nutrition & Integrative Physiology, Florida State University College of Health and Human Sciences, Tallahassee, FL, USA. [5]Wake Forest University, Winston Salem, Winston Salem, NC, USA. [6]Department of Genetics, University of North Carolina School of Medicine, Chapel Hill, NC, USA. [7]Department of Microbiology and Immunology, Emory University School of Medicine, Atlanta, GA, USA. e-mail: mzafar@wakehealth.edu; mazafar@emory.edu

pneumoniae[3,8–10]. Antibiotic treatment in a hospital setting is associated with *K. pneumoniae* expansion in the gut and subsequent development of diseases such as pneumonia, bacteremia, pyogenic liver abscesses, and urinary tract infections[11,12]. *K. pneumoniae* is a major threat to patient health and places a significant burden on the healthcare system[13,14]. Despite the pathologies associated with *K. pneumoniae* infection, it is considered a pathobiont because the initial gut colonization event is generally asymptomatic[15,16].

Although *K. pneumoniae* primarily has been associated with immunocompromised patients, recent studies suggest that up to 30% of the population in a community setting can be colonized with *K. pneumoniae*[17–20], indicating an adeptness in overcoming microbiome-mediated CR. Resident gut microbiota generally mediate CR against incoming microorganisms either through exploitation competition (limiting nutrient resources)[21–23] or interference competition (direct inhibition through antimicrobial toxins)[24–27]. We recently described a murine model of *K. pneumoniae* gut colonization with an intact resident gut microbiome[28]. Using this model, we demonstrated that *K. pneumoniae* resides in the gut asymptomatically and metabolizes fucose to overcome CR[29]. We also observed that colistin-resistant *K. pneumoniae* has a defect in gut colonization, which is alleviated by an antibiotic-mediated reduction in microbiome complexity[30]. Furthermore, recent studies have demonstrated that gut commensals, such as *Bacteroidetes* priming the host immune system and *K. oxytoca* depleting preferred carbohydrate sources[31,32], provide CR against *K. pneumoniae*. Nevertheless, these examples are not comprehensive, and *K. pneumoniae*-gut microbiota interactions still need to be further investigated.

In this study, we leveraged our murine model of *K. pneumoniae* gut colonization with a high throughput approach (transposon mutagenesis) to identify *K. pneumoniae* factors (genes) that allow it to overcome CR in an unbiased manner[33,34]. Many of the genes that were identified encode factors that are either involved in alternative nutrient utilization or modification of the bacterial surface, suggesting that *K. pneumoniae* requires these pathways to overcome both host- and microbiota-mediated CR. One such factor was the type VI secretion system (T6SS). We established that the T6SS promotes *K. pneumoniae* GI colonization in the presence of an intact microbiota, that expression of the T6SS genes is tightly regulated by conditions known to be prevalent in the gut lumen and identified regulatory mechanisms not previously reported that control expression. A subsequent metagenomics screen identified key interacting partners of *K. pneumoniae* in the gut, including *Betaproteobacteria* species that we demonstrated to be targeted by *K. pneumoniae*. As the gut serves as a likely reservoir for *K. pneumoniae*, our study identifies the key factors that support *K. pneumoniae* colonization and interactions with the resident gut microbiome.

Results

Identification of genes that promote *K. pneumoniae* gastrointestinal colonization

To identify genes that contribute to *K. pneumoniae* GI colonization, we generated a *mariner* transposon library of random mutants in the strain KPPR1S that contained 56,757 unique insertions in open reading frames, approximating a 10-fold coverage of the genome (Fig. S1). Our input library contained 68 genes with no transposon inserts and 120 genes with only 1 insert, suggesting that these genes likely are essential for *K. pneumoniae* growth in broth culture. Next, we assessed bottleneck effects (stochastic loss of mutants) and appropriate dosing by inoculating mice with a mixture of distinct antibiotic-resistant isolates of KPPR1S[35] at several ratios and determined the competitive indices (CI) from fecal shedding at day 7 post inoculation (dpi). We observed high variability in the CI for mice inoculated with 1:10,000 compared to 1:1000 and other mixtures, suggesting that there was no detectable stochastic loss of either strain when inoculated at 1:1000 (Fig. S2A). Thus, an inoculum of 10^9 CFU containing ~5000 mutants was considered appropriate to overcome bottleneck effects for transposon-insertion sequencing (INSeq) studies. Nine independent pools were each inoculated into two mice (biological replicate; $n = 18$ mice total). Feces were collected and plated daily to determine colonization density and to ensure that the mice were sufficiently colonized. At 7 dpi, the ceca were harvested for DNA extraction (library output); DNA was also extracted from the inoculum (library input). Input and output DNA was sequenced and analyzed using DESeq2 and TnseqDiff[36,37] to determine the essentiality of the sequenced genes. Details on the generation, isolation, and analysis of the INSeq libraries are described in the Methods section.

Using the arbitrary cutoff of adjusted P value of <0.05, 470 of 5159 annotated genes[38] (9.11%) significantly contributed to the ability of *K. pneumoniae* to colonize a murine GI tract with an intact microbiome (Fig. 1A, Supplementary Data 1). Many of the genes associated with GI colonization fall into functional pathways associated with nutrient uptake and metabolism, suggesting a competition for resources in the gut (Fig. 1B). Herein, we focused on genes encoding membrane-associated proteins as these are most likely to impact host-microbe and microbe-microbe interactions (Table 1). These include genes encoding proteins involved in lipopolysaccharide synthesis and modification, transporters for metal ions, capsular polysaccharide synthesis, secretion systems, and nutrient transporters.

The T6SS of *K. pneumoniae* is a colonization determinant

Among the subset of candidates predicted to encode membrane-associated proteins were seven that encode key structural components of a T6SS (Fig. 1A, Table 1), suggesting a potential role for this molecular machinery in the colonization of the GI tract. T6SS are generally involved in contact-dependent inhibition of other gram-negative bacterial species[39]. KPPR1S encodes two annotated T6SS loci and three auxiliary clusters (Fig. 1C). One locus (T6SS-1) is closely related to the T6SS loci present in *K. variicola* strain At-22, the hypervirulent *K. pneumoniae* strain NTUH-K2044[40], and the classical *K. pneumoniae* isolate CH1157, whereas the second locus (T6SS-2) appears to only have similarity to the T6SS-2 of the classical isolate CH1157[41,42]. However, the regions encoding the effector-immunity pairs in both loci are specific to KPPR1S. Using Bastion6 and SecReT6, we identified the putative effector-immunity pairs within each locus[43,44]. In T6SS-1 we identified a putative type VI lipase effector with homology to Tle1 that was shown to target the cell membranes[45]. It contains a DUF2235 domain, which is generally associated with VgrG and proline-alanine-alanine-proline (PAAR) repeat-containing proteins[45–47]. *K. pneumoniae* Tle1 from CH1157 was shown to be functionally active against laboratory *E. coli*[41]. In T6SS-2 locus we identified three effector proteins, two distinct phospholipase D (homology to PldB1 and 2), and a PAAR domain containing effector protein[48] (Fig. S3). The putative effectors from T6SS-2 locus have not been functionally characterized under in vitro or in vivo conditions.

To ascertain whether the predicted *t6ss* genes (genes encoding T6SS proteins collectively will be designated '*t6ss*') are expressed in the GI tract, qRT-PCR was performed using *K. pneumoniae* specific primers and RNA isolated from the ceca of mice inoculated with KPPR1S. The first gene from each of the T6SS loci (*tssB* [T6SS-1], *tssK2* [T6SS-2]) were upregulated compared to M63 minimal media grown cultures (Fig. 1D). Additionally, we cloned the promoter regions from each T6SS locus into a *gfp* reporter plasmid (T6SS-1, pPROBE-*tssB'-gfp*$^+$ and T6SS-2, pPROBE-*tssK2'-gfp*$^+$). Mice were inoculated with KPPR1S containing these plasmids, and fluorescence measured from bacteria isolated from the cecum 24 h post inoculation (hpi). Compared to the control medium (M63), expression of *tssB* and *tssK2* were ~7-fold and ~3-fold higher, respectively (Fig. S2B). Collectively, our

https://doi.org/10.1038/s41467-025-56309-8

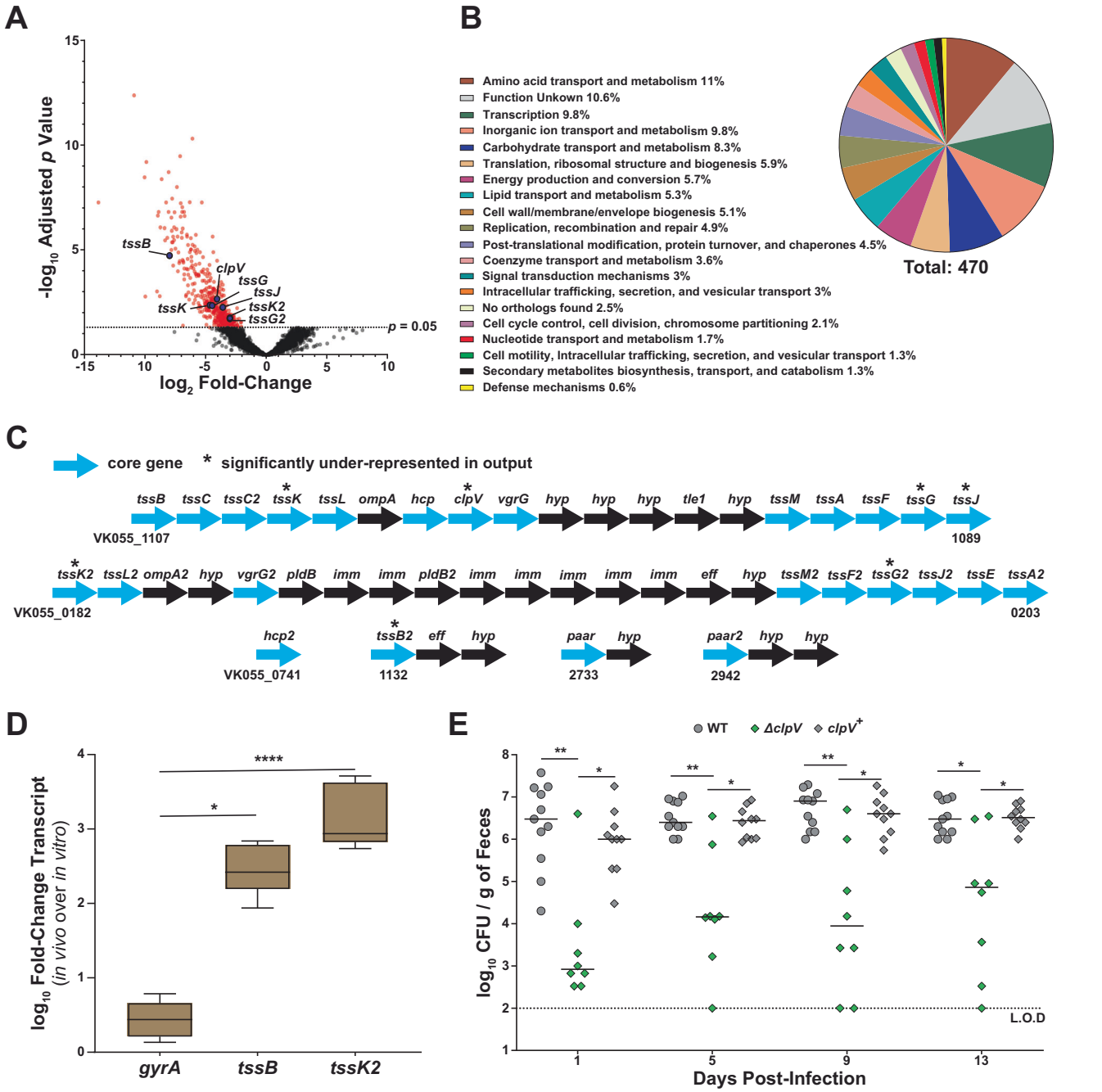

Fig. 1 | An INSeq approach identified the T6SS as a major contributor to *K. pneumoniae* gut colonization. A Genome-wide changes as observed through a volcano plot from Tn-seq studies comparing in vitro grown mutants (input) to mutants isolated from the cecum of infected mice (output). Fitness differences are shown as fold-change on the x-axis with the adjusted *p*-value using the Benjamini-Hochberg Procedure on the y-axis. All of the significant genes for gut colonization are highlighted in red, the T6SS genes are in blue. **B** Pie chart showing the distribution of the functional pathways of the proteins encoded by the genes identified in (**A**). **C** The genetic organization of the T6SS loci in *K. pneumoniae* strain KPPR1S with the locus tag underneath. Core genes (blue) are those required for the assembly, structure, and firing of the T6SS. Asterisks represent genes with transposon insertions that led to defect in gut colonization. *hyp*, hypothetical; *eff*, effector; *imm*, immunity. Putative effector-immunity pairs were identified using Bastion6 and SecReT6. **D** qRT-PCR showing the expression of gyrase (*gyrA*) and genes from the T6SS loci in the GI tract using *K. pneumoniae* specific primers. Displayed is the fold-change in transcript of *gyrA*, *tssB*, and *tssK2* RNA extracted from either cecal contents of *K. pneumoniae* infected mice ($n = 3$) or RNA extracted from *K. pneumoniae* grown in M63 minimal media. *rrsA* (16S) was used as the housekeeping gene for calculating $2^{-\Delta\Delta C_T}$ using KPPR1S-specific primers. Boxes and whiskers indicate the median and the minimum and maximum values, respectively. A two-tailed Kruskal-Wallis test with Dunn's post-test was performed. *p*-values from left to right: 0.0232, <0.0001. **E** Fecal shedding from mice infected with either the WT ($n = 10$), the isogenic Δ*clpV* mutant ($n = 8$), or the chromosomally complemented strain (*clpV*$^+$) ($n = 10$). Feces were collected from inoculated mice on the indicated days. Each symbol indicates a single mouse, the bars indicate median CFU and the dashed line indicates the limit of detection (L.O.D). A two-tailed Kruskal-Wallis test with Dunn's post-test was performed. There was no significant difference between WT and *clpV*$^+$ at any time point. *p* values from left to right: 0.0014, 0.034, 0.0028, 0.016, 0.0024, 0.0168, 0.029, 0.0230. *, $p < 0.05$; **, $p < 0.01$; ****, $p < 0.0001$.

Table 1 | Membrane-associated factors identified in the INSeq screen

VK55 #	*p* adj value	Gene name[a] and description	Function	Reference
1132	6.41E-08	*tssb*, T6SS structural protein	Component of the contractile sheath of the T6SS	52
4232	1.16E-07	*fimA*, type-1 fimbrial protein, A chain	Structural subunit of the major fimbriae	133
1928	2.47E-06	*fepD*, ferric enterobactin transport system permease protein	Component of ABC transporter complex FepBDGC for the uptake of enterobactin	134
5125	0.0008	*ybtX*, putative cytoplasmic transmembrane protein	Yersiniabactin-associated zinc MFS transporter	135
1100	0.0009	*clpV*, T6SS protein	ATPase responsible for disassembly of the T6SS contractile sheath after firing	52
5086	0.0010	*virB8*, type IV secretion system protein	Component of the type IV secretion system inner membrane complex	136
0627	0.0031	*nikE4*, nickel import ATP-binding protein	ATP binding component of the NikABCDE Ni^{2+} ABC transporter complex	137
0360	0.0035	Iron complex transport system permease protein	*fecCD* transport family protein, involved in translocation of Fe^{3+} across the membrane	138
1104	0.0041	*tssk*, T6SS structural protein	Component of the baseplate complex of the T6SS	52
0627	0.0075	*nikE*, nickel import ATP-binding protein	ATP binding component of the NikABCDE Ni^{2+} ABC transporter complex	137
1399	0.0087	*lpxL2*, lipid A biosynthesis lauroyltransferase	Transfers laurate to the KDO_2-lipid IV_A, one of the final steps in KDO_2-lipid A synthesis	139
3623	0.0091	*arnB*, UDP-L-Ara4O C-4′ transaminase LPS modification	Modifies lipid A phosphates with 4-amino-4-deoxy-L-arabinose, increasing resistance to polymyxin	140
1543	0.0151	*msbA*, ATP-dependent lipid A-core flippase	Translocation of lipid A-core from the inner leaflet to the outer leaflet of the inner membrane	141
4412	0.0176	*nlpD*, activator of cell wall hydrolase AmiC	Necessary for daughter cell separation during cell division	142
1089	0.0181	*tssJ*, T6SS structural protein	Component of the membrane complex of the T6SS	52
1602	0.0134	*potH*, putrescine transport system permease protein	Part of the ABC transporter complex PotFGHI for putrescine import	143
0260	0.0190	*oppC*, oligopeptide transport system permease protein	Component of the binding-protein-dependent transport system for oligopeptides	138
0393	0.0268	*ccmA*, cytochrome c biogenesis ATP-binding export protein	Component of ABC transporter complex CcmAB involved in biogenesis of c-type cytochromes	144
1090	0.0312	*tssG*, T6SS structural protein	Component of the baseplate complex of the T6SS	52
4890	0.0326	*mgtE*, magnesium transporter	Selective magnesium channel important for Mg^{2+} homeostasis	145
5012	0.0485	*galF*, UTP-glucose-1-phosphate uridylyltransferase	Translocation and surface assembly of capsular polysaccharide	146

The *p-values* were then adjusted for multiple testing using the Benjamini-Hochberg Procedure.
[a]Listed gene names are in italics.
A two-sided *p-value* was provided using TnseqDiff[37]

expression studies suggest that *K. pneumoniae t6ss* expression is regulated, with conditions prevalent in the gastrointestinal tract promoting robust expression.

ClpV, an ATPase identified in our INSeq screen (Fig. 1A, Table 1), is involved in disassembling the T6SS contractile sheath, allowing the system to reassemble for repeated use. Recently ClpV was demonstrated to be required for robust gut colonization by *K. pneumoniae* isolate KP52.415 both with and without antibiotic treatment in a sodium bicarbonate treatment model of *K. pneumoniae* gut colonization[49]. However, gastric acid serves as a major bottleneck to host infection by enteric pathogens, and its neutralization by sodium bicarbonate consequently modulates pathogen infectivity[50,51]. Therefore, we generated a *ΔclpV* mutant in KPPR1S and tested the ability of this strain to colonize the gut in our murine model of *K. pneumoniae* GI colonization, where host bottlenecks are not manipulated[28]. Over the course of the study (15 days) mice inoculated with the *ΔclpV* strain shed poorly compared to mice inoculated with wild type KPPR1S (WT) strain (Fig. 1E). Additionally, we observed lower burden of the *ΔclpV* strain in the GI tract, including the oropharynx and the lower intestinal sites (Fig. S2C, D). The complemented strain, with *clpV* introduced at the native site (*clpV*$^+$), shed as robustly as WT, validating that the defect was specific to the deletion of *clpV* (Fig. 1E, Fig. S2C, D). Interestingly, during co-inoculation studies, the WT strain was able to compensate for the GI colonization defect of the *ΔclpV* strain (Fig. S2E, F), suggesting that the mutant acts as a social cheater, relying on the functional T6SS of the WT strain to promote robust gut colonization. Overall, these results validate the INSeq screen and confirm that the T6SS of *K. pneumoniae* is required for robust colonization of the murine GI tract with an intact microbiota.

Both T6SS loci are required for robust GI colonization

KPPR1S T6SS-1 has 12 of the 13 genes that encode core structural components of the T6SS, lacking only the gene *tssE* that encodes a base plate component, whereas T6SS-2 has nine of the 13 conserved core genes annotated, lacking *tssB* and *tssC* that encode the contractile sheath components, *clpV* that encodes the sheath disassembly enzyme and *hcp* that encodes the syringe tubule component[52] (Fig. 1C). Additional copies of *hcp* and *tssB* are present in two of the auxiliary clusters, and both T6SS loci encode unique effector-immunity pairs (Fig. 1C, Fig. S3)[53]. To investigate whether *K. pneumoniae* requires one or both T6SS loci for gut colonization, we generated strains with deletions of the entire T6SS-1 locus (T6−/+), T6SS-2 (T6+/−) locus, or both T6SS-1 and T6SS-2 loci (T6−/−) and tested them in our murine model. These locus mutants lack the T6SS structural genes and the effector immunity pair genes from the respective locus. The mice inoculated with the T6−/+, T6+/−, and T6−/− all had low fecal shedding burden compared to the WT (Fig. 2A), and reduced colonization density in the GI tract (Fig. S4A, B). The single locus mutants (T6−/+, T6+/−) had similar defects in shedding, whereas the double locus mutant (T6−/−) appeared to have a more severe defect in shedding over the course of the study. This indicates that both loci contribute to *K. pneumoniae* gut colonization.

https://doi.org/10.1038/s41467-025-56309-8

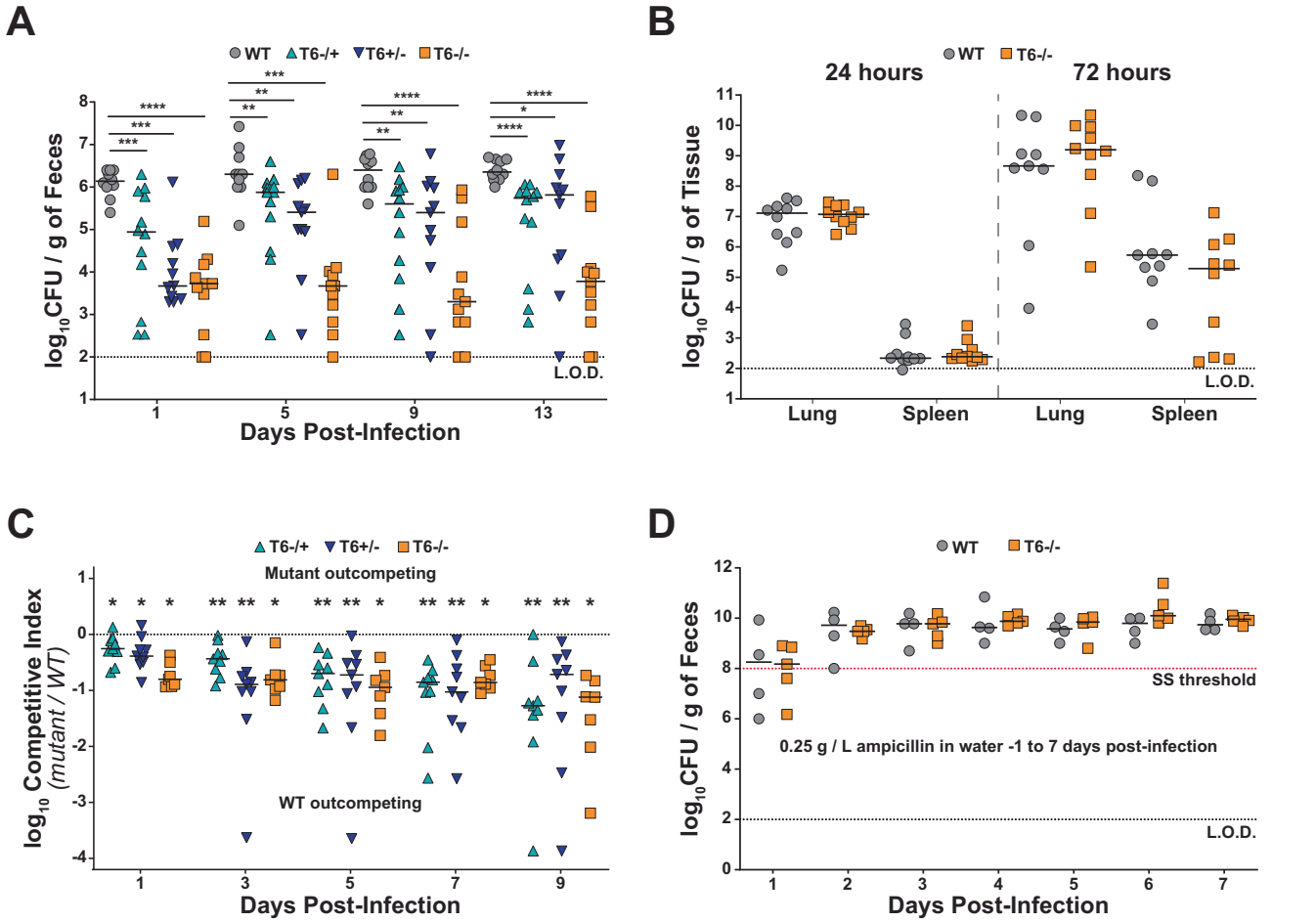

Fig. 2 | Both T6SS loci of *K. pneumoniae* are important for gut colonization. **A** Fecal shedding of *K. pneumoniae* infected mice. Mice were orally infected with 10^6 CFU of either the WT($n = 10$), T6−/+ (locus 1 deletion) ($n = 12$), T6+/− (locus 2 deletion) ($n = 11$), or T6−/− (double deletion) ($n = 11$). Two-tailed Mann-Whitney *U* test was used to compare the WT to each mutant on a given day for statistical analysis. *p*-values from left to right: 0.0002, 0.0001, <0.0001, 0.0074, 0.0019, 0.0001, 0.0018, 0.008, <0.0001, <0.0001, 0.0148, <0.0001. **B** Colonization of lungs and spleens from *K. pneumoniae* infected mice. Mice were infected intranasally with 10^4 CFU of either WT or T6−/− and tissues were collected at 24 or 72 h post-infection (WT 24 h: $n = 10$, T6−/− 24 h: $n = 10$, WT 72 h: $n = 9$, T6−/− 72 h: $n = 10$). A two-tailed Mann-Whitney *U* test was performed between the WT and the T6−/− at each time point and no significant differences were identified. **C** Fecal shedding from in vivo competition studies. Mice were orally infected with a 1:1 mixture of WT and T6−/+ ($n = 9$), T6+/− ($n = 9$), or T6−/− ($n = 7$). Each point represents the $\log_{10}$ competitive index value from an individual mouse on the indicated day, the bars indicate the median competitive index (CI), and the dotted line indicates a CI of 1. The CI was determined as described in Methods. One sample Wilcoxon signed-rank tests were performed for each group against a theoretical value of 0. *p*-values from left to right: 0.0195, 0.0117, 0.0156, 0.0039, 0.0039, 0.0156, 0.0039, 0.0039, 0.0156, 0.0039, 0.0039, 0.0156, 0.0078, 0.0039, 0.0156. **D** *K. pneumoniae* fecal burden from antibiotic-treated mice inoculated with either the WT ($n = 4$) or the T6−/− strain ($n = 5$). Mice were given 0.25 g/L ampicillin in their drinking water beginning 24 h prior to inoculation and for the duration of the experiment. The red dashed line indicates the super-shedder threshold (≥10^8 CFU [SS Threshold]). A two-tailed Mann-Whitney *U* test was performed between the WT and the T6−/− at each time point and no significant differences were identified. For graphs (**A** and **D**), *, $p < 0.05$; **, $p < 0.01$; ***, $p < 0.001$; ****, $p < 0.0001$. In graphs (**A**, **B**, and **D**) each symbol represents tissue from a single mouse, the bars indicate median bacterial burden, and the dotted line indicates the L.O.D.

A signature-tagged mutagenesis screen in KPPR1 showed that T6SS mutants did not survive in the lung, and an ST258 lineage *K. pneumoniae* isolate was shown to have upregulated T6SS gene expression during lung infection[54,55]. However, neither study validated their genome-wide screens by testing *t6ss* mutants in vivo. Consequently, we tested whether the T6SS of KPPR1S is required for lung colonization. Mice were inoculated via the intranasal route with either the WT or T6−/− strain and colonization density was enumerated from the lungs and spleens at 24 and 72 hpi. Interestingly, we did not observe any differences between the T6−/− and the parental strain in their ability to colonize the lung or spleen (Fig. 2B), suggesting that the T6SS is dispensable for the colonization of, and dissemination from, the lungs.

Next, as the *ΔclpV* defect in gut colonization was rescued by the WT strain during coinfection (Fig. S2E, F), we sought to ascertain whether the loss of either or both loci would result in a similar social cheater phenotype. However, the WT strain was unable to rescue the colonization defect of the single and double T6SS locus mutants (Fig. 2C, Fig. S4C), indicating that the effector-immunity proteins encoded within the loci are critical for robust gut colonization. Additionally, a coinfection performed with the single locus mutants (T6−/+ & T6+/−) showed that neither mutant had an advantage over the other (Fig. S4D), signifying that both loci are important for *K. pneumoniae* gut colonization.

As our results show that the T6SS only appears to benefit *K. pneumoniae* in the GI tract and not in the lung, which has a less complex microbiota[56,57], we hypothesized that the defect in gut colonization is due to CR mediated by the more complex microbiota of the GI tract. Thus, we tested the ability of T6SS mutant strain (T6−/−) to colonize the GI tract of mice treated with ampicillin to deplete the

microbiota[58]. We previously observed that mice on antibiotic treatment develop a supershedder phenotype (>10^8 CFU/g of feces), where *K. pneumoniae* shed in the feces from the antibiotic-treated group is ~100-fold greater than that of mock-treated mice[28,30,59]. Both the WT and T6−/− strain developed a supershedder phenotype in antibiotic-treated mice (Fig. 2D); the WT and T6−/− strain colonized mice at a similar level indicating that the reduced microbiota in the antibiotic-treated mice effectively lowered the CR such that T6−/− could establish colonization. Collectively, our results show that to overcome microbiota-mediated CR, *K. pneumoniae* deploys the T6SS, allowing it to thrive in the dynamic environment of the GI tract.

K. pneumoniae t6ss genes are directly regulated by ArgR, FNR, and Fur in response to GI-specific growth conditions

Expression of *t6ss* is often tightly regulated due to the metabolic cost of synthesizing this complex machinery[53,60]. As our data indicated that the *t6ss* genes are more highly expressed in the mouse GI tract than in M63 minimal media (Fig. 1D), we hypothesized that environmental cues in the gut trigger the expression of *t6ss* genes. Examination of the promoter regions of both *t6ss-1* and *t6ss-2* revealed putative binding sequences for ArgR (arginine metabolism), Fur (iron homeostasis) and FNR (anaerobic growth)[61] (Fig. 3A). We also observed upregulation of genes known to be regulated by ArgR (*astC*, succinylornithine transaminase; arginine catabolism), Fur (*fepD*, enterobactin ABC transporter; iron acquisition) and FNR (*ssuE*, FMN reductase; sulfur utilization)[62–64] in the GI tract, suggesting that conditions in the gut are conducive for these regulators to be active (Fig. S5A). Furthermore, *astD* (*ast* operon member), *fepD,* and *ssuE* were also identified to be important gut colonization determinants in our INseq approach. To test the role of these regulators on *t6ss* expression more directly, we first conducted qRT-PCR using RNA isolated from *K. pneumoniae* grown in either arginine-rich media (+Arg), anaerobic conditions (-O_2), or iron-depleted media (-Fe), to determine whether these three environmental signals alter the expression of representative *t6ss* genes. Under each condition, both *tssB* (T6SS-1) and *tssK2* (T6SS-2) were upregulated 2-4-fold (Fig. 3B).

We next sought to examine the effects of ArgR, Fur, and FNR on *t6ss* regulation by measuring the GFP expression levels from the *tssB′-gfp*$^+$ transcriptional fusion in WT, *ΔargR*, *fnr::cam*, and *fur::cam* mutant strains. When grown in M63 with arginine, GFP levels in WT were 2-fold higher than in M63 lacking arginine, whereas no change was observed in the *ΔargR* strain (Fig. 3C). A similar trend was observed when grown anaerobically, where GFP levels were 3-fold higher in WT, but no change in expression in the *fnr::cam* strain (Fig. 3D). Likewise, a 2-fold increase in GFP was observed from in WT grown with 2, 2′-Dipyridyl (DIP), and no change between iron replete vs DIP in the *fur::cam* strain (Fig. 3E). However, there was a slight increase in expression comparing *tssB* in WT and *fur::cam* in iron replete conditions, indicating that Fur functions as a repressor. Similar dependencies on growth medium and regulators were also observed for expression of the *tssK2* promoter (*tssK2′-gfp*$^+$) (Fig. S5B–D). Thus, environmental conditions consistent with those in the GI tract led to increased expression of genes from both T6SS loci, and this change required the presence of the condition-responsive regulators ArgR, FNR and Fur.

While these expression data provide evidence of a requirement for ArgR, FNR, and Fur for expression of the T6SS genes, they are not evidence of direct regulation. We therefore conducted DNA-protein-interaction enzyme-linked immunosorbent assays (DPI-ELISA) to determine if the regulatory effects are direct or indirect. We first tested biotinylated DNA oligomers selected from promoters of genes known to be bound and regulated by each transcription factor (*astC* for ArgR; *ssuE* for FNR; and *fepD* for Fur[62–64]). Each fragment showed the expected binding specificity, indicating that our purified proteins were active (Fig. S5E–G). We then designed DNA oligomers from the *tssB* promoter region containing one of the predicted binding motifs (test) (Fig. 3A) or scrambled sequences (control)[65–67]. We observed significantly more protein binding to the test fragments than to the control fragment, demonstrating ArgR, FNR, and Fur directly bind the *tssB* promoter (Fig. 3F–H). Competitive DPI-ELISA assays with Fur and increasing concentrations of either non-biotinylated test or control oligomer demonstrated the specificity of the DNA-protein interactions. Increasing concentration of competitive test oligomer reduced Fur binding to the streptavidin bound oligomer, whereas increasing concentration of control did not impact Fur-DNA interaction, providing evidence that the interactions observed are specific (Fig. S5H–J). Collectively, our results demonstrate that *K. pneumoniae t6ss* genes are tightly regulated through specific transcriptional factors that respond to environmental cues present in the gastrointestinal tract.

Metagenomic analyses reveal that *K. pneumoniae* triggers changes in the gut microbiome

A previous study using streptomycin treated mice demonstrated that *K. pneumoniae* modulated the gut microbiome potentially in a T6SS-dependent manner[41]. These antibiotic treated mice had reduced microbial diversity, thus allowing an incoming pathogen to more easily overcome CR[41]. To provide insight into changes that occur when *K. pneumoniae* is introduced into the gut with an intact microbiota, and to understand early colonization interactions between *K. pneumoniae* and the resident gut microbiome, we performed a shotgun metagenomics screen on fecal pellets obtained from mice prior to inoculation and at 2, 4 and 7 dpi with the WT isolate(KPPR1S). No significant alterations in the relative abundance of the microbiome were detected between pre- and post-infection, in either the bacterial or fungal genera (Figs. 4A, S6A). We examined alpha diversity to ascertain if there were changes in the diversity of the microbiota that included the chao1 index (an indicator of total richness) (Fig. 4Bi), the Shannon index (measures abundance and evenness of species) and Simpson index (measures number and relative abundance of each species) (Fig. 4Bii, iii), and performed a principal component analysis (PCA) between the infected and uninfected cohort. We also calculated the Firmicutes/Bacteroidetes (F/B) ratio as these groups represent two of the largest phyla present in the gut[68]. Changes in the F/B ratio due to *K. pneumoniae* gut colonization would suggest microbial imbalance. None of these tests indicated any significant differences in diversity, F/B ratio nor a correlation between the infection status and the relative abundance of the genera identified in the screen (Fig. 4C, Fig. S6B). The lack of significant shifts in the microbiota is consistent with the observed asymptomatic colonization of *K. pneumoniae*, as significant disruptions generally accompany inflammation and gut dysbiosis[69].

While we did not detect major shifts in the microbiome composition at a higher order between inoculated and uninoculated mice, a Spearman correlation analysis on the relative abundance of bacterial strains ($n = 123$) identified specific changes in the microbiota and identified putative *K. pneumoniae* interacting partners (Supplementary Data 2). Among the strains ($n = 17$) that were reduced following *K. pneumoniae* colonization were the gram-negative bacteria Oscillibacter *sp. 1-3* (*Oscillibacter*), *Burkholderiales bacterium 1_1_47* (*Burkholderiales*), and *Parasutterella excrementihominis YIT 11859* (*Parasutterella*) (Fig. 4D). The family *Oscillospiraceae* had previously been identified as a likely target of T6SS of *K. pneumoniae*[41], supporting our results. These organisms could serve as prey targeted by the T6SS of *K. pneumoniae*. Taken together, our microbiome sequencing results demonstrate that even though there are no major shifts in microbiome composition, there are modulations at the strain level associated with *K. pneumoniae* gut colonization, and that *Betaproteobacteria* species that are affected by *K. pneumoniae*.

https://doi.org/10.1038/s41467-025-56309-8

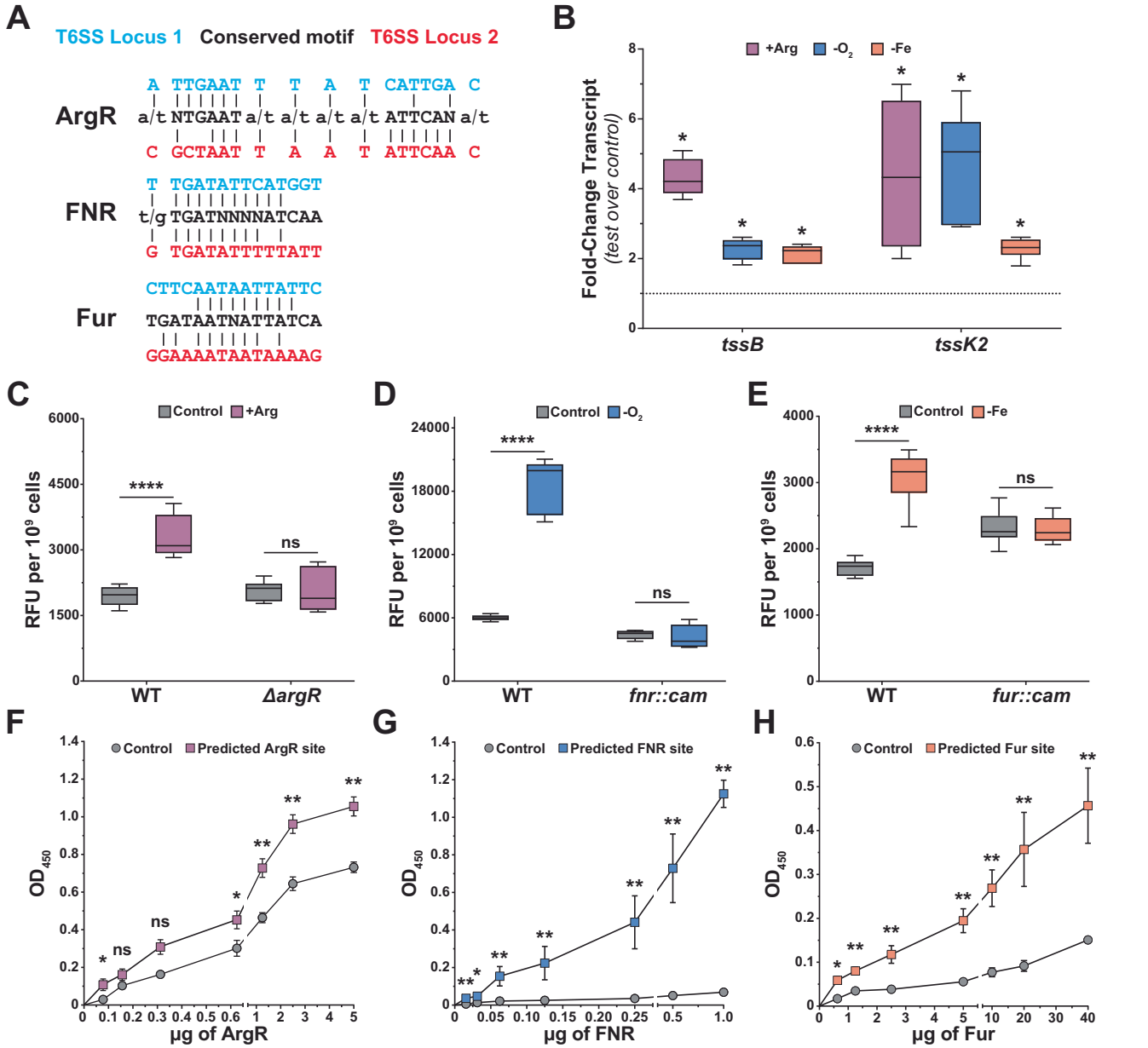

Fig. 3 | ArgR, FNR, and Fur modulate the expression of the *t6ss* genes. A The putative binding motifs for ArgR, FNR, and Fur at the T6SS promoter regions compared to the consensus sequences. **B** qRT-PCR analysis of KPPR1S grown in conditions corresponding to the activity each of the transcriptional regulators compared to M63. Shown is the fold-change in transcript levels of *tssB* (locus 1) and *tssK2* (locus 2) from strains grown in M63 or M63 with arginine (+Arg), in LB media aerobically or anaerobically ($-O_2$), and in LB media with or without 200 mM 2,2′-dipyridyl (-Fe). $n = 3$ biological replicates. One sample Wilcoxon signed rank tests against a theoretical value of 1 was performed for each target gene under each test condition. p-values from left to right: 0.0312, 0.0312, 0.0312, 0.0312, 0.0312, 0.0312. **C**–**E** ArgR, FNR, and Fur are required for *t6ss* expression. WT and isogenic regulator mutants containing pPROBE-*tssB′-gfp*$^+$ were grown in their respective test and control conditions. The relative fluorescent units (RFU) were normalized to 10^9 CFU. $n = 3$ biological replicates. (F-H) DPI-ELISA used to show that ArgR, FNR, and Fur bind their predicted sites in the T6SS-1 promoter. Purified 6xHis-tagged transcription factors were added to wells coated with DNA oligomers with either the predicted binding sequence or control DNA with a scrambled sequence. Binding was detected using an HRP-conjugated anti-poly-histidine antibody. Absorbance values (OD_{450}) depict binding of protein to adhered DNA. Shown are the mean +/− SEM at each concentration. $n = 2$ biological replicates for each recombinant protein with 7 different concentrations tested in triplicate. **C**–**H** Two-tailed Mann-Whitney U tests were performed to determine the significant differences between the control and experimental samples. p values from left to right: **C** < 0.0001, 0.9133 **D** < 0.0001, 0.3401, **E** < 0.0001, 0.7304, **F** 0.0317, 0.2381, 0.0556, 0.0317, 0.0079, 0.0079, 0.0079, **G** 0.0079, 0.0317, 0.0079, 0.0079, 0.0079, 0.0079, 0.0079, **H** 0.0159, 0.0079, 0.0079, 0.0079, 0.0079, 0.0079, 0.0079.*, $p < 0.05$; **, $p < 0.01$.

K. pneumoniae colonization reduces *Parasutterella* in the gastrointestinal tract

Parasutterella and *Burkholderiales* have been isolated from the healthy human gastrointestinal tract[70], but they remain poorly characterized genetically because of difficulty in culturing them[71]. Thus, to ascertain whether *K. pneumoniae* affects *Parasutterella* levels in the murine gut, we utilized droplet digital PCR (ddPCR). ddPCR allows for the absolute quantification of a specific nucleotide target sequence by separating a more traditional quantitative PCR (qPCR) reaction into thousands of individual reactions, in this case by microfluidic oil emulsion of a reaction volume[72]. DNA was isolated from the feces of mice pre-inoculation and at 2, 4, and 7 dpi with either the WT or the T6−/− strain. ddPCR was conducted using species-specific primers and dual labeled fluorescent probes (Supplementary Data 3). To account for shedding and

https://doi.org/10.1038/s41467-025-56309-8

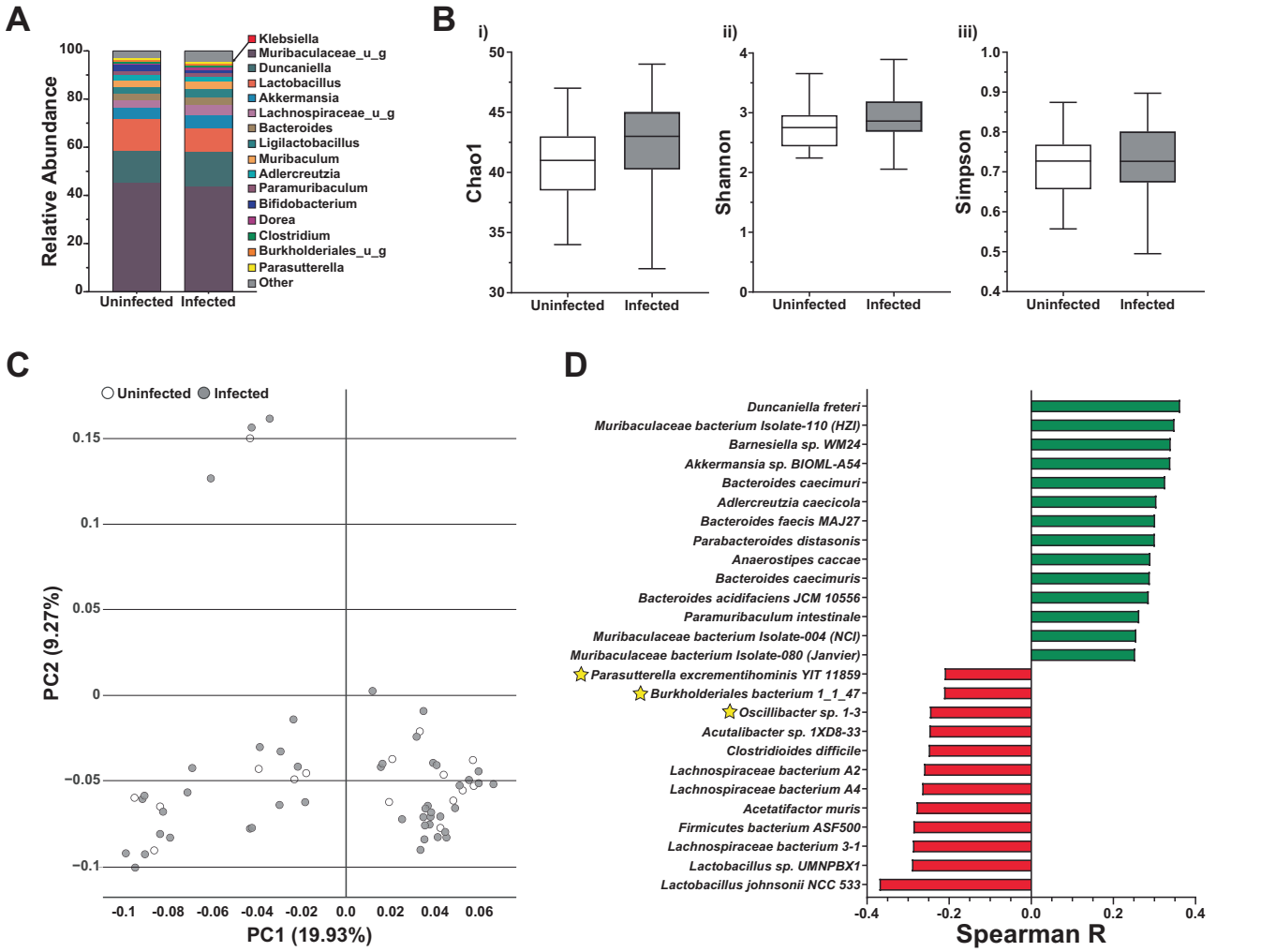

Fig. 4 | Shotgun metagenomics analyses identifies *K. pneumoniae*-associated modulation of the gut microbiome. Shotgun metagenomics sequencing was conducted on fecal samples from mice 24 h before and days 2, 4, and 7 post-oral inoculation with *K. pneumoniae* ($n = 16$). **A** Intestinal microbiota content pre- and post-inoculation as percent relative abundance of major genera. **B** Alpha diversity index (i) Chao1, (ii) Shannon, and (iii) Simpson analyses of mice pre- or post-inoculation. Boxes and whiskers indicate the means and the minimum to maximum values, respectively. **C** PCA of metagenomics data by the attribute of relative abundance. **D** Spearman ranks of selected bacterial strains in the microbiome following inoculation. Spearman rank-order correlation coefficient test was performed between the gut microbiome strains before and after infection. Stars represent the gram-negative bacterial strains that were reduced.

colonization differences between the WT and T6−/− strains, the copies of the target in a sample were normalized to *K. pneumoniae* CFU from feces of the corresponding mouse. Our results showed that *Parasutterella* levels from mice inoculated with the WT strain were significantly reduced, whereas no reduction was observed in the T6−/− inoculated mice (Fig. 5A). Additionally, the calculated rate of decline of *Parasutterella* was significantly higher in the samples from WT inoculated mice than that from the T6−/− inoculated mice (Fig. 5B). Additionally, we conducted ddPCR on a species that was not impacted by *K. pneumoniae* gut colonization (*Duncaniella sp. B8* [Spearman $R = 0.00019$]). We observed no change in *Duncaniella* between pre- and post-inoculation with mice inoculated with either the WT or the T6−/− mutant (Fig. 5C, D), indicating that *K. pneumoniae* gut colonization does not impact this commensal organism. Thus, these data are consistent with the metagenomics screen data and demonstrate either a direct or an indirect link between *K. pneumoniae* T6SS function and the depletion of *Parasutterella*.

GI-specific growth conditions promote *K. pneumoniae* T6SS dependent interbacterial competition

Even though expression of the *t6ss* genes in *K. pneumoniae* is upregulated in vitro under gut mimetic growth conditions (presence of arginine, low iron and oxygen levels) (Figs. 3B–E, S5B–D), it is possible that this system is also regulated post-translationally, as was observed in *P. aeruginosa*[73]. Therefore, we sought to determine whether the *K. pneumoniae* T6SS is functionally active under the conditions where *t6ss* gene expression was upregulated by performing in vitro killing assays. We used a *Burkholderia cepacia* isolate as a proxy for *Parasutterella* and *Burkholderiales*, as they are difficult to culture in vitro. *B. cepacia* is a *Betaproteobacteria* species closely related to *Parasutterella* and *Burkholderiales*, is easy to culture, and has multiple antibiotic resistance markers that allow for differentiation from *K. pneumoniae*. We did not observe any significant killing of the *B. cepacia* (prey strain) when incubated with *K. pneumoniae* grown in M63 minimal medium (Fig. 6A), consistent with our finding that the *t6ss* is expressed only at low levels in this growth condition. In contrast, when *K. pneumoniae* was grown in each of the three gut mimetic conditions, we observed killing of the prey strain (Fig. 6A). This reduction in *B. cepacia* survival was T6SS-dependent, as we observed no reduction in *B. cepacia* survival when co-incubated with the T6−/− strain grown in the test conditions (Fig. 6A). Combining multiple conditions of anaerobiosis with arginine did not yield increased killing of the prey strain compared to either single condition (Fig. S7A).

https://doi.org/10.1038/s41467-025-56309-8

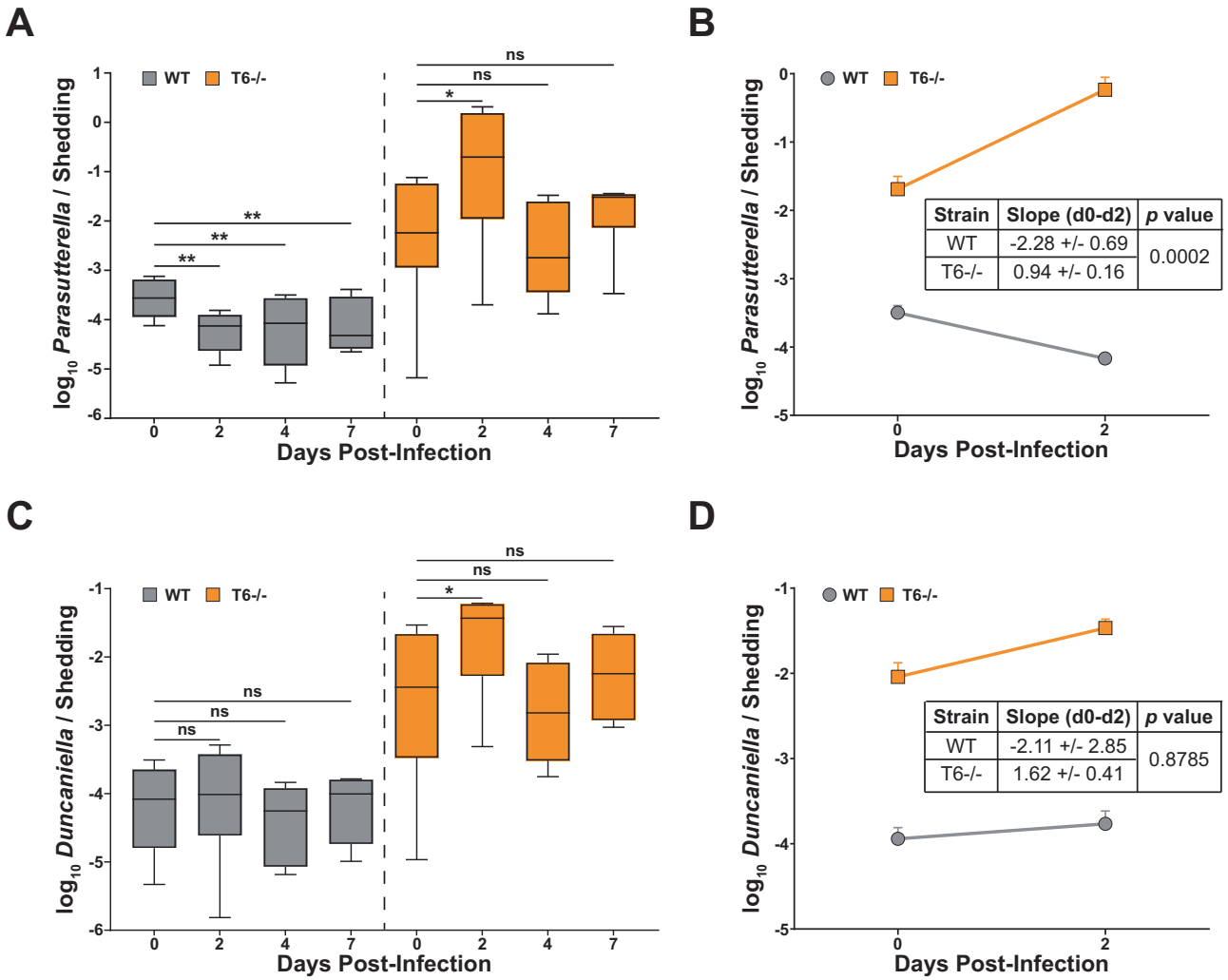

Fig. 5 | *K. pneumoniae* reduces *Parasutterella* from the gut in a T6SS-dependent manner. For absolute quantification of bacterial levels, droplet digital PCR (ddPCR) was performed on DNA extracted from fecal pellets of mice 24 h pre-infection and days 2, 4, and 7 post-inoculation with the WT or the T6SS−/− strain ($n = 4$ for each group). **A**–**D** *Parasutterella* and *Duncaniella* were quantified from each sample and then adjusted to the *K. pneumoniae* shedding on each given day to account for potential effects from the reduced colonization levels of T6−/− infected mice. Pre-infection (day 0) sample was adjusted to the average *K. pneumoniae* shedding from the same mouse on days 2, 4, and 7 post-inoculation to serve as a baseline for comparison. **A** *Parasutterella* levels in the murine GI tract following inoculation with WT or T6−/−. **B** Change in *Parasutterella* levels between days 0 and 2. **C** *Duncaniella* levels in the murine GI tract following inoculation with WT or T6−/−. **D** Change in *Duncaniella* levels between days 0 and 2. **A**, **C** A two-tailed Friedman test followed by Dunn's multiple comparison test was performed comparing days 0, 2, 4, and 7 for WT and for T6−/− samples. Boxes and whiskers indicate the median and the minimum to maximum values, respectively. Adjusted p values from left to right: **A** 0.0058, 0.0058, 0.0058, 0.0201, 0.7358, 0.364, **C** > 0.9999, 0.2441, >0.9999, 0.0201, 0.7358, 0.364. **B**, **D** Shown are the mean +/− SEM values at day 0 and 2 post-infection, the tables indicate the average of the slopes for the samples from each mouse from day 0 to 2 post-infection, along with the standard error. Two-tailed Mann-Whitney U tests were performed to determine the statistical difference between the slopes. *, $p < 0.05$; **, $p < 0.01$.

To ascertain if these T6SS phenotypes were unique to KPPR1S or more generally applicable to other *K. pneumoniae* strains, we tested another hypervirulent strain, hvKP1[74] in the interbacterial competition assay. When grown under the gut mimetic conditions, hvKP1 exhibited killing of *B. cepacia* that was T6SS specific, as a hvKP1 *ΔclpV* mutant did not kill the prey strain (Fig. 6B). In addition, interbacterial killing assays with KPPR1S and a commensal *E. coli* or the gram-positive *Ligilactobacillus animalis*, (both isolated from the GI tract of mice in our facility) did not lead to any significant reduction of these murine gut commensal strains (Fig. S7B). This suggests that under the conditions tested, multiple *K. pneumoniae* strains use the T6SS to target specific prey strains. However, unlike *Acinetobacter baumannii*[75], it does not appear to target gram-positive bacteria. These data demonstrate that the arginine-rich, low oxygen, and low iron conditions prevalent in the GI tract directly upregulate the transcription and promote activity of the *K. pneumoniae* T6SS, leading to killing of *Betaproteobacteria* (Fig. 7).

Discussion

Worldwide, over 1 million deaths are attributed annually to antibiotic-resistant bacteria[76]. *K. pneumoniae* is a key nosocomial pathogen and gastrointestinal carriage of antibiotic-resistant *K. pneumoniae* is considered a major risk factor for subsequent systemic infection[77,78]. Thus, to identify the factors that contribute to *K. pneumoniae* GI colonization, we conducted an INSeq screen using our murine model of *K. pneumoniae* gut colonization with an intact microbiota. With this approach, we identified 470 genes important for *K. pneumoniae* gut colonization, among which were several encoding components of a T6SS. We validated the INSeq screen by showing that the T6SS of *K. pneumoniae* is critical for gut colonization in the presence of an intact

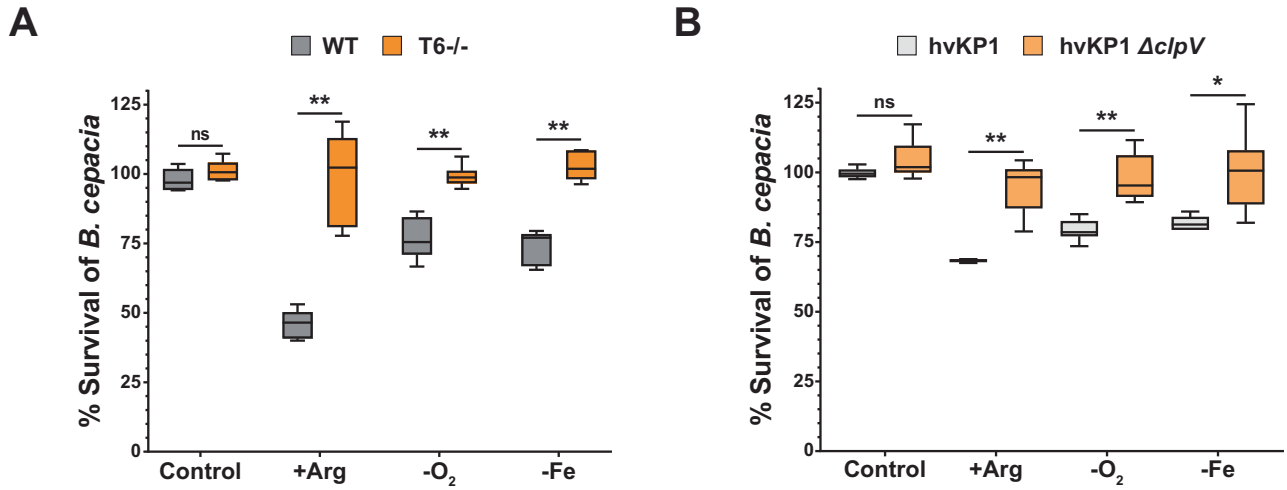

Fig. 6 | Betaproteobacteria member *Burkholderia cepacia* is reduced by *K. pneumoniae* in a T6SS-specific manner. A–**B** KPPR1S (WT), hvKP1 (hypervirulent isolate) and the corresponding mutant strains were incubated with *B. cepacia* to assess T6SS-dependent killing. *K. pneumoniae* was grown in M63 (control), M63 with arginine as the nitrogen source (+Arg), anaerobically (-O_2), or M63 with 200 mM 2,2′-dipyridyl (-Fe). *B. cepacia* was gown in LB. The *K. pneumoniae* and *B. cepacia* cultures were mixed at a 1:1 ratio, or with PBS only, and incubated on LB agar plates at 37 °C for 2 h. Percent survival was calculated by dividing the CFU of each strain from the competition mixture (*K. pneumoniae* + *B. cepacia*) by the CFU from non-competition mixture (*B. cepacia* alone or *K. pneumoniae* alone). *B. cepacia* on average was reduced from 1.04e^7 to 4.7e^6 (+Arg), 5.86e^7 to 4.39e^7 (-O_2) and 6.37e^6 to 4.72e^6 (-Fe), with KPPR1S acting as a predator. $n = 3$ biological replicates. Boxes and whiskers indicate the median and the minimum to maximum values, respectively. Two-tailed Mann-Whitney *U* tests were performed to determine the significant differences between the control and experimental groups. *p*-values from left to right: **A** 0.132, 0.0022, 0.0022, 0.0022, **B** 0.132, 0.0022, 0.0022, 0.0152. ns = not significant, *, $p < 0.05$, **, $p < 0.01$.

microbiota and that its expression is upregulated during infection and under gut mimetic growth conditions in vitro. While other transposon mutagenesis screens led to identification of *K. pneumoniae* factors important for lung infection[54,79] and GI colonization in an antibiotic-treatment model (ablating the gut microbiome and the associated CR)[80,81], this screen differs in that we identified genes that contribute to *K. pneumoniae* GI colonization using a more natural context with an intact microbiome. In addition to genes that encode the T6SS machinery, our screen identified genes that encode for enzymes involved in ethanolamine (EA) metabolism (Supplementary Data 1), which we recently demonstrated to be critical for *K. pneumoniae* gut colonization[82], further validating our mutagenesis screen[82].

One way an incoming microorganism can overcome CR is through direct killing of microbiota members that occupy the same metabolic niche[83]. The T6SS provides gram-negative bacteria the ability to kill specific bacterial species, allowing the predator species to take over the niche[84–87]. T6SSs have also been implicated in biofilm formation, metal ion acquisition, and quorum sensing, all of which could promote GI colonization[88]. However, disruption of the gut microbiota with antibiotic treatment resulted in robust colonization of both the WT and the T6SS double locus deletion mutant (Fig. 2D). These data suggest that the primary role of the *K. pneumoniae* T6SS is to carve out a niche by reducing competing bacterial population.

The complexity and host-to-host variability of the gut microbiota pose significant challenges to detecting and characterizing specific pathogen-microbiota interactions[1,2]. This variability can also influence the ability of enteric pathogens to establish colonization[89,90]. The gut metagenomics analysis identified *K. pneumoniae* interacting partners. At the genus level, we did not observe major shifts in the microbiome following inoculation with *K. pneumoniae* (Fig. 4A). However, there was a reduction in *Firmicutes* and an increase in *Bacteriodetes*, and these changes have been associated with gut dysbiosis[68]. At the species level, we identified gram-negative, but not gram-positive, bacterial species that were depleted following *K. pneumoniae* colonization (Fig. 4D). We focused on the closely related organisms, *Burkholderiales* and *Parasutterella*, as they are both in the class *Betaproteobacteria* that encompasses many human pathogens. Although previous studies with enteric pathogens have shown that some deploy a T6SS against commensal bacteria isolated from the GI tract[84,86,87], it is difficult to ascertain whether these isolated bacteria are truly physiologically relevant prey partners. To achieve a more direct measurement of T6SS-mediated depletion of a prey species in vivo, we utilized ddPCR to enumerate the amount of *Parasutterella* in mouse fecal samples pre- and post-inoculation with either the WT or T6−/− *K. pneumoniae and* demonstrated a T6SS-dependent reduction of *Parasutterella* (Fig. 5A, B). Additionally, in vitro killing assays with the related *Betaproteobacteria*, *B. cepacia*, showed that *K. pneumoniae* can kill members of this class in a T6SS-dependent manner (Fig. 6A, B). Interestingly, our results and those from Sana et al.[87], show that *E. coli* is immune to *K. pneumoniae* and *Salmonella enterica serovar Typhimurium* T6SS activity (Fig. S7B). The findings are contrary to the results obtained with *Vibrio cholerae*, which was observed to kill commensal *E. coli* isolates[84], suggesting that *E. coli* isolates have immunity against the T6SS activity of certain pathogenic bacteria, and these isolates could be employed to bolster CR against incoming pathogens. The *S. Typhimurium* T6SS did not act on gram-positive commensal bacteria[87], suggesting that the *K. pneumoniae* and *S. Typhimurium* T6SSs likely are only effective against gram-negative bacterial species.

It is hypothesized that the synthesis and assembly of the T6SS is associated with high biological cost[60] which manifests as tight transcriptional regulation. We observed higher expression of the *t6ss* genes in the gut compared to growth in broth culture (Figs. 1D, S2B), suggesting that there are environmental signals in the GI track that dictate T6SS expression. Expression of *t6ss* is frequently tightly controlled, but the signals and mechanisms of regulation among different species vary significantly[53,60]. Previous studies have implicated a diverse set of conditions and transcriptional regulators that modulate the expression of *t6ss* genes in other bacteria; these conditions include changes in pH, oxygen tension, presence of bile salts, and antimicrobial peptides that are prevalent in the gut[53,91–95]. In examining the promoter regions for the *K. pneumoniae t6ss* loci, we identified putative binding sites for three transcription factors, ArgR, FNR, and Fur, that respond to conditions found in the GI tract: high arginine, a hypoxic environment, and competition for iron (low iron), respectively[96–98]. Fur is known to regulate *t6ss*

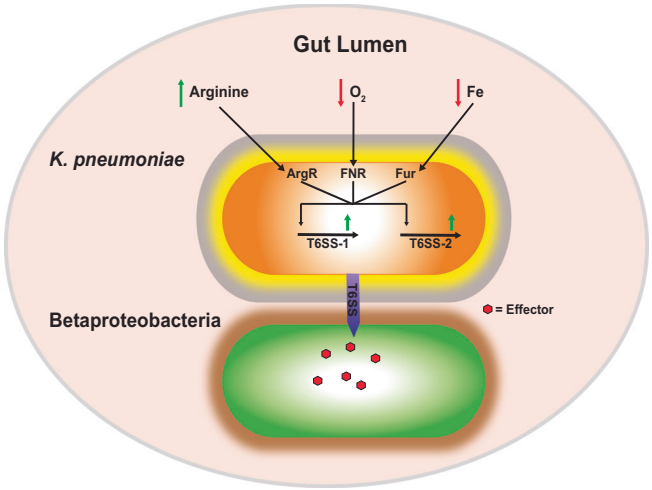

Fig. 7 | Regulatory effects induced by the gastrointestinal tract environment on *K. pneumoniae*, leading to T6SS-mediated killing of Betaproteobacteria. The gut lumen is an anaerobic environment, where there is intense competition for nutrients such as iron (Fe), and carbon and nitrogen sources; arginine can serve as an alternative nitrogen source. All three conditions (+Arg, low O_2, low Fe) act as cues, and through their respective regulators (ArgR, FNR, and Fur) modulate the expression of *K. pneumoniae t6ss* genes. *K. pneumoniae* uses its T6SS against *Betaproteobacteria* species. The reduction of this population presumably frees up essential nutrients that *K. pneumoniae* needs to propagate. This propagation can result in asymptomatic colonization, but also promote dissemination to other organs that lead to dangerous disease manifestations.

genes in other species[60,99–101], but direct regulation of *t6ss* genes by FNR has only been demonstrated in an avian pathogenic *E. coli* isolate[102], and there is no current evidence of direct regulation by ArgR. Because arginine is a poor nitrogen source, the alternate sigma factor for nitrogen stress (RpoN) is likely active in the gut, and it has been shown to modulate *t6ss* expression in *K. pneumoniae* and other species[95,103,104]. Thus, we speculate that ArgR functions in conjunction with RpoN to upregulate the expression of *K. pneumoniae t6ss* genes. Enteric pathogens such as *V. cholerae* cause gut dysbiosis that leads to elevated oxygen levels[105,106]. This likely explains why expression of the pandemic *V. cholerae t6ss* genes is not activated under anaerobiosis[107], whereas *K. pneumoniae* senses the hypoxic environment of the gut to activate the T6SS.

There are several caveats to the approach used in our INSeq screen. First, we used only a single laboratory-adapted strain (KPPR1S). *K. pneumoniae* genomes are highly plastic and strains fall broadly into two different pathotypes[17,108]; differences in genomic content could lead to strain-to-strain variability in gut colonization. Yet, in vitro competition between another *K. pnemoniae* strain (hvKP1) and *B. cepacia* suggests the T6SS is key for this strain to overcome CR as well. Second, even though mice and humans share similarities in their microbiomes[109] there are key differences that could affect the ability of *K. pneumoniae* to colonize the intestinal tracts. However, we did identify interacting partners that are shared between human and murine gut microbiomes, suggesting these results may extrapolate to human colonization. Third, random transposon insertions could occur such that they only partially abrogate the function of a gene or cause polar effects, and our analysis pipeline (TnseqDiff) only takes into account insertions that occur somewhere within the coding sequence of a gene. Lastly, the role of *trans*-acting factors such as siderophores would be masked when random mutants are tested *en masse*. Such mutants known as social cheaters, are able to use factors produced by other mutants that they cannot synthesize. Despite these caveats, the findings from transposon mutagenesis screen were independently tested and validated the results of our INSeq screen.

Our findings herein add to the list of bacterial factors and environmental signals that regulate the expression of T6SSs and identify specific predator-prey interactions. Based on our observations, we propose a model that illustrates the multiple regulatory elements that control the expression of the *K. pneumoniae t6ss* genes (Fig. 7). Three regulators, in response to known environmental conditions in the gut, control *t6ss* gene expression, of which ArgR had not previously been shown to participate in *t6ss* regulation. Under gut mimetic growth conditions in vitro, increased *t6ss* gene expression led to increased T6SS-dependent killing of *Betaproteobacteria* that were confirmed to be target species in vivo. Taken together, our study demonstrates there is a complex set of environmental cues present in the GI tract that manifest in the activation of the T6SS. This allows *K. pneumoniae* to shape the resident gut microbiota and carve out a niche in the gut from which it can spread systemically and cause disease.

Methods

All experiments comply with the ethical regulations at Wake Forest School of Medicine. This study was conducted according to the guidelines outlined by the National Science Foundation animal welfare requirements and the Public Health Service Policy on Humane Care and Use of Laboratory Animals[110]. All animal work was done according to the guidelines provided by the American Association for Laboratory Animal Science (AALAS)[111] and with the approval of the Wake Forest Baptist Medical Center Institutional Animal Care and Use Committee (IACUC). The approved protocol numbers for this project are A20-084 and A23-064.

Strain and plasmid construction

Primers are listed in Supplementary Data 3. Strains, and plasmids used in this study are listed in Tables S1, and S2, respectively. All mutants are routinely tested for capsule production, hypermucoviscosity, and biofilm formation. The *ΔclpV*, *ΔargR*, and hvKP1 *ΔclpV* mutants (AZ117, AZ251, and AZ310) were generated using λ red recombinase to replace the gene with a kanamycin resistance cassette (kan) from pKD4; pKD46 contains the recombinase genes[79]. Transformants were selected on kanamycin plates (25 μg/mL) and confirmed by PCR. Removal of the kan cassette was accomplished using pFlp3[112]. Chromosomal complementation of the *ΔclpV* mutant (AZ184) was achieved with pKAS46-based allelic exchange, as previously described[30,113].

To generate the *fur* and *fnr* gene and deletion mutants (AZ187 and AZ188, respectively), the target regions were amplified from mutants in MKP103 (AZ181 and AZ182, respectively)[114]. The PCR products were integrated onto the chromosome via λ red recombination[79], selected on LB agar with chloramphenicol (50 μg/mL), and confirmed by PCR. To introduce the apramycin resistance gene into the T6−/+ and T6+/− mutants (AZ246, and AZ247, respectively), the cassette from the *attTn7* site of AZ94[35] was amplified and integrated onto the chromosome via λ red recombination[79]. Following selection on apramycin (50 μg/mL), candidates were confirmed by PCR.

Deletions of the *t6ss* loci were generated by allelic exchange using pKAS46[113]. Briefly, ~800 bp regions up and downstream of each locus were amplified and cloned into pKAS46. The resulting plasmids (pCB057, pCB090) were transformed into *E. coli* S17-1 λ pir and conjugated into KPPR1S as described[115]. Following selection on LB with rifampin/kanamycin and counterselection on streptomycin (2500 μg/mL), candidates were screened by PCR to identify deletion mutants.

To generate kan-resistant clones of the T6−/+ and T6+/− mutants, each strain was transformed with pUC18R6K-mini-Tn7T-Km and pTNS2 as described[116] to integrate the *kan* cassette at the *attTn7* site. Following selection on LB plates with kanamycin, candidate clones were confirmed by PCR.

To generate *gfp* transcriptional fusions, ~500 bp fragments encompassing target promoter regions were amplified from KPPR1S and cloned into pPROBE[117] using NEBuilder assembly (NEB). The

resulting plasmids (T6SS-1, pPROBE-*tssB′-gfp*$^+$ and T6SS-2, pPROBE-*tssK2′-gfp*$^+$) were transformed into S17-1 λ pir, selected on kanamycin plates, and confirmed by sequencing. The plasmids were then electroporated into target *K. pneumoniae* strains as described[118].

The *argR*, *fnr*, and *fur* genes were amplified from KPPR1S, cloned into pET28a to generate 6xHis-tagged versions of each regulator (*pET28a-argR, pET28a-fnr, pET28a-fur)*. The Q5 Site-Directed Mutagenesis Kit (NEB) was used with the *pET28a-fnr* construct to introduce the D154A mutation that allows FNR to function under aerobic conditions[119]. Each plasmid was confirmed by sequencing.

Mouse infections and bacterial shedding

Specific-pathogen-free C57BL/6J mice were obtained from Jackson Laboratory (Bar Harbor, ME) and were bred and maintained (~18–23 °C with a 12 h light/dark cycle and ~45% humidity) in the animal facility at Biotech Place, Wake Forest Baptist Medical Center on standard chow and water *ad libitum*. 5- to 7-week-old male and female mice (equal number) were inoculated orally with 100 μL containing 10^6 CFU of *K. pneumoniae* suspended in phosphate-buffered saline (PBS) + 2% sucrose from a pipette. For coinfections, mice were infected with a 1:1 ratio of 10^6 CFU of each of the specified *K. pneumoniae* isolates. Fecal and organ collection was carried at indicated time points, homogenized, and plated on appropriate antibiotic plates to enumerate bacterial colonization[28,30]. The limits of detection were 10^2 CFU/gram of sample for fecal and organ homogenate samples, and 33 CFU/mL for oral lavage. The competitive index (CI) was calculated as $\log_{10}$ ((mutant output/WT output)/(mutant input/WT input)).

For lung inoculations, mice were anesthetized by intraperitoneal (i.p.) injection with ketamine/xylazine and inoculated with 2×10^4 CFU as described[115]. At indicated time points, mice were euthanized, lungs and spleens removed, homogenized, and plated on appropriate antibiotic plates to enumerate bacterial colonization.

Transposon library and INSeq screen

The transposon mutant libraries were generated as described by Bachman et al.[79]. Two mice each were infected with a pool containing ~5000 mutants at a dose of 10^9 CFU. Feces were collected from the mice for 6 days to ensure they were robustly colonized (~10^6 CFU/g feces). On day 7 post-infection, the mice were euthanized and a portion of the cecal homogenate was plated to determine end-point colonization. The remaining homogenate (output sample) was subjected to insertion sequencing[34]. The input samples were taken from the inoculum preparation given to the mice. Samples were sequenced using Illumina Hiseq (1 × 50 Rapid Run) and analysis was carried out using DESeq2 and TnseqDiff[36,37]. Nine independent inoculations were carried out for a total of nine inputs and eighteen outputs.

GFP reporter assays

Plasmids containing the T6SS promoter-*gfp* fusions were transformed into *K. pneumoniae* strains of interest. For in vitro assays, saturated cultures grown overnight in M63 minimal media with 0.5% glucose (M63, Control) at 37 °C were subcultured 1:100 into fresh media for expression analysis. For anaerobiosis (-O_2), cultures in anaerobically adjusted media were placed in an anaerobic chamber (Coy Lab Products) and grown to an OD_{600} of 0.5. For iron depletion (-Fe), 200 μM 2,2′dipyridyl (DIP) was added to the M63, and cultures were grown at 37 °C to an OD_{600} ~ 0.2. As the *ΔargR* strain has a growth defect with arginine supplied as a nitrogen source, the overnight cultures were diluted 1:100 into fresh M63, grown to an OD_{600} of ~0.5, washed, and then switched to M63 media with 0.2% arginine instead of ammonium sulfate (+Arg) and grown for an additional two hours. For each test condition, strains were also grown in control M63 to the same OD_{600}. At the desired endpoint, the bacteria were pelleted and adjusted to OD_{600} = 1.0 in PBS. To overcome the necessity of oxygen for GFP fluorescence, anaerobic cultures were pelleted and resuspended in PBS, then aerated for 24 h at 37 °C with agitation. Relative fluorescence units were measured at 80 gain using a Synergy H1 plate reader (BioTek). The RFU values were normalized to CFU.

To examine *t6ss-gfp* expression in vivo, mice were inoculated with either AZ216 (KPPR1S + pPROBE-*tssB′-gfp*$^+$) or AZ220 (KPPR1S + pPROBE-*tssK2′-gfp*$^+$), and feces and ceca were harvested at 24 hpi. The cecal samples were suspended in PBS, centrifuged briefly at a low speed (1000 × *g*, 30 s) to pellet large debris, the supernatant was moved to a new tube and the centrifugation repeated. The supernatant was then transferred to a new culture tube and kanamycin (25 μg/ml) was added. The samples were then aerated to provide oxygenation for GFP folding by continuous agitation at 37 °C for 24 h.

To examine *t6ss-gfp* expression ex vivo, strains carrying either a reporter plasmid or vector were grown in cecal filtrate (CF) with 25 μg/ml kanamycin; the CF was prepared as previously described[29]. The cultures were grown aerobically with continuous agitation at 37 °C. After 24 h, the cultures were pelleted, resuspended in an equal volume of PBS + 25 μg/ml kanamycin, and aerated by continuous agitation at 37 °C for 24 h. Control samples were grown in M63 and similarly processed.

RNA isolation, DNA synthesis, and qRT-PCR

Isolation of KPPR1S RNA from in vitro samples was performed using TRIzol reagent[120] with modifications[29]. For +Arg conditions, cultures were grown in M63 control overnight, then subcultured (1:100) into fresh M63 (control) or M63 +Arg, grown to OD_{600} = 0.5, followed by RNA extraction. For the anaerobic (-O_2) and iron chelated (-Fe) samples, cultures were grown in LB-Lennox broth (LB) aerobically overnight, subcultured (1:100) into either LB (control), or LB with 200 μM DIP (-Fe), or LB and moved to an anaerobic chamber (Coy Lab Products). The -O_2 samples were grown to OD_{600} = 0.5, and the -Fe samples were grown to OD_{600} = 0.1, at which time the RNA was isolated. RNA was isolated from the cecal contents as described[121] with modifications[29]. Total RNA from all samples was treated with DNase (Invitrogen; AM1907) followed by cDNA synthesis (iScript™, BIO-RAD)[120]. qRT-PCR was conducted[122,123] using *K. pneumoniae* species-specific primers[29]. 16S rRNA served as the reference gene with primers specific to *K. pneumoniae*. Expression was quantified via the $\Delta\Delta C_T$ threshold cycle (C_T) method[122]. Fold-change was calculated using $2^{-\Delta\Delta C}{}_T$[29].

Protein purification

BL21(DE3) (AZ47) carrying *pET28a-argR* and *pET28a-fur* were grown overnight in LB with 50 μg/mL of kanamycin, subcultured into 200 ml of expression media (LB, 50 μg/mL kanamycin, and 10.3 μL of Antifoam A [Sigma-Aldrich]) and grown at 37 °C with constant agitation until they reached ~0.6 OD_{600}, then treated with 0.5 mM Isopropyl ß-D-1-thiogalactopyranoside (IPTG). BL21 (DE3) (Δ*crp, Δfnr*)[119] carrying pET28a-*fnr-D154A* that encodes a functionally active form of FNR under aerobic conditions[119,124] was grown similarly as above, except the LB was supplemented with 0.2% glucose. The bacteria were collected by centrifugation, and the pellet was weighed and stored at −80 °C.

Bacterial pellets were resuspended in lysis buffer (IMAC buffer [NEB], 5% glycerol, 0.5% Triton X-100, 10 mM 2-mercaptoethanol, 2 mg/ml lysozyme, and 50 μl/g Protease Inhibitor Cocktail [Sigma-Aldrich]; 5 mL per 1 gram of pellet), incubated at room temperature for 5 min, then chilled on ice for 10 min. Bacterial suspensions were sonicated 10X (Branson Sonifier 250; 30 s on, 30 s off, 20% output), then centrifuged (12,000 × *g*, 15 min, 4 °C) to remove cell debris. The supernatant was passed through a 0.45 μm filter to further remove debris and intact bacteria. Protein purification was then carried out using the NEBExpress Ni Spin Column Kit (NEB) with a high salt wash buffer (50 mM Imidazole, 500 mM NaCl, 50 mM NaH_2PO_4, pH 8) to reduce non-specific binding. The final elution buffer was exchanged for a storage buffer (10 mM Tris-HCl, 100 mM NaCl, 5% glycerol, pH 8) using Amicon Ultra-4 Centrifugal Filters with a 10 kDa cutoff

(Millipore). To confirm protein purity in the elution sample, an aliquot was run on 12% polyacrylamide gel (Bio-Rad) and stained with Simply Blue SafeStain (Invitrogen). Protein concentration was measured via Bradford assay.

DNA protein interaction (DPI) ELISA

DPI-ELISAs[125] were carried with the following modifications: The DNA-oligomers (2 pmol) containing specific binding motif or scrambled sequence were bound to streptavidin-coated plates via incubation for 2 h at room temperature with gentle agitation. Each wash step was repeated 4x with 200 μl of PBS. The blocking solution volume and duration were increased to 150 μL and 1 h, respectively. The purified His-tagged proteins were diluted to various concentrations tested in blocking buffer (5% BSA in PBS) and incubated as recommended[125]. Anti-His mouse monoclonal HRP conjugate antibody (Thermo Scientific; MA1-21315-HRP) was diluted 1:1000 in PBS and developed using 100 μL/well of 1-Step Slow TMB-Elisa Substrate Solution (Thermo Scientific) for 15 min at room temperature. The reaction was stopped with the addition of 100 μL per well of 0.18 M H_2SO_4 and the OD_{450} was then measured.

Competitive DPI-ELISAs experiments were conducted to test for protein binding specificity. Purified His-tagged Fur was used at a concentration of 20 μg per well containing the biotinylated DNA-oligomer (2 pmol) containing the Fur binding motif from *tssB* promoter region bound to streptavidin coated plates. Competing non-biotinylated oligomers that either contained the Fur binding motif or the scrambled sequence were added at a concentration of 0.1X, 1X and 10X of the bound biotinylated DNA-oligomer. Incubation and detection were performed as described above.

Metagenomics screen

Fecal samples were collected from mice at days 0, 2, 4, and 7 post-infection with WT *K. pneumoniae*, as described above. DNA was extracted from the fecal samples using the Qiagen PowerSoil Pro kit and quantified using a Qubit (ThermoFisher). DNA libraries were prepared using the Illumina Nextera XT library preparation kit, assessed using Qubit (ThermoFisher), and run on an Illumina HiSeq platform 2 × 150 bp.

For the bioinformatic analysis of the metagenomic data, unassembled sequencing reads were directly analyzed by the CosmosID bioinformatics platform (CosmosID Inc., Rockville, MD)[126–129] for multi-kingdom microbiome analysis, profiling of antibiotic resistance, virulence genes, and quantification of relative organism abundance. The resulting species-level taxonomic profiles were used to calculate the Shannon and Chao1 diversity indices using the microbiome 'R' package (http://microbiome.github.com/microbiome)[130], and the Bray-Curtis dissimilarity index-based beta-diversity was assessed using the phyloseq 'R' package[131]. Spearman's rank correlation coefficient was utilized for correlational analysis (Supplemental Data 2).

Droplet digital PCR (ddPCR)

Absolute quantification of *Parasutterella* and *Duncaniella* was conducted as previously described[132] with the following modifications: Fecal pellets were collected from mice infected with either WT or T6−/− *K. pneumoniae* at days 0 (pre-infection) and 2, 4, and 7 post-infection, and DNA was isolated using the PowerFecal Pro DNA kit (QIAGEN). Reaction mixes were prepared in 96-well plates (Bio-Rad) with each reaction containing 2 μL (900 nM) of each primer, 2 μL (250 nM) of the dual-labeled probe, 5 μL of the sample DNA (0.5 ng/μL dilution used with *Parasutterella* and *Duncaniella*), and 11 μl of ddPCR Supermix for Probes (no dUTP, Bio-Rad). Plates were loaded into an Automated Droplet Generator (Bio-Rad), and the subsequent droplet samples were amplified using a C1000 Touch Thermal Cycler (Bio-Rad). After amplification, the plate was placed in a QX200 Droplet Reader (Bio-Rad) and the read conditions were set using QuantaSoft software (Bio-Rad). All samples were quantified on two separate runs. To correct for the differing levels of *K. pneumoniae* colonization in each mouse, the concentration (copies/μL) of *Parasutterella*, and *Duncaniella* were divided by the CFU of *K. pneumoniae* per gram feces from the corresponding sample. For day 0, the shedding value was set as the average shedding of the corresponding mouse on days 2, 4, and 7 post-infection. This method was chosen as the difference between the normal shedding and limit of detection (L.O.D.) on the log scale would heavily skew the day 0 adjusted values, making comparisons inaccurate.

Interbacterial killing assay

Predator *K. pneumoniae* strains were grown overnight in M63 and diluted in PBS to OD_{600} = 4.0. For the control group, the strains were subcultured 1:100 in fresh M63. For the test groups, predator strains were subcultured 1:100 in +Arg, -Fe, or -O_2 media, then grown for 24 h at 37 °C. The prey strains were grown in LB (*B. cepacia* and *E. coli*) or De Man-Rogosa-Sharpe (MRS) broth (*L. animalis*) at 37 °C. Afterward, the predator and prey strains were each adjusted to OD_{600} = 1.0 in PBS, then an equal volume of the predator and prey strains were mixed together (competition), predator and PBS (predator non-competition), and prey and PBS (prey non-competition). 20 μL of each mixture were spotted onto separate nitrocellulose membrane filters (0.45 μm, Millipore), placed onto an LB agar plate, and incubated at 37 °C for 2 h. The incubation time was selected based on growth kinetics of both the predator and prey isolates. Bacteria were dislodged from the membranes by vortexing in 1 mL of PBS for 1 min, then serial diluted and plated on appropriate media for enumeration. *K. pneumoniae* strains were selected on LB with streptomycin (500 μg/mL), *B. cepacia* on LB with trimethoprim (5 μg/mL), *E. coli* on TBX agar, and *L. animalis* on MRS plates. Percent survival was calculated by dividing the CFU of each strain from the competition mixture by the CFU from non-competition mixture.

Statistical analysis

All statistical analyses were performed using Prism 9.0 (GraphPad Software, Inc., San Diego, CA), except Metagenomics and Tn-Seq screen sections (see details above). Data were analyzed with the Mann-Whitney *U* test (comparing two groups), the Kruskal-Wallis test with Dunn's post-test, Friedman's test with Dunn's post-test, or the Wilcoxon signed-rank test.

Reporting summary

Further information on research design is available in the Nature Portfolio Reporting Summary linked to this article.

Data availability

The sequencing data have been deposited to the NCBI SRA repository, under the accession PRJNA1190643. Raw data, materials, and reagents are available upon request. Source data are provided with this paper.

References

1. Lozupone, C. A., Stombaugh, J. I., Gordon, J. I., Jansson, J. K. & Knight, R. Diversity, stability and resilience of the human gut microbiota. *Nature* **489**, 220–230 (2012).
2. Bull, M. J. & Plummer, N. T. Part 1: the human gut microbiome in health and disease. *Integr. Med.* **13**, 17–22 (2014).
3. Kim, S., Covington, A. & Pamer, E. G. The intestinal microbiota: antibiotics, colonization resistance, and enteric pathogens. *Immunol. Rev.* **279**, 90–105 (2017).
4. Pickard, J. M., Zeng, M. Y., Caruso, R. & Núñez, G. Gut microbiota: role in pathogen colonization, immune responses, and inflammatory disease. *Immunol. Rev.* **279**, 70–89 (2017).
5. Buffie, C. G. & Pamer, E. G. Microbiota-mediated colonization resistance against intestinal pathogens. *Nat. Rev. Immunol.* **13**, 790–801 (2013).
6. Pop, M. et al. Diarrhea in young children from low-income countries leads to large-scale alterations in intestinal microbiota composition. *Genome Biol* **15**, R76 (2014).

7. Singh, P. et al. Intestinal microbial communities associated with acute enteric infections and disease recovery. *Microbiome* **3**, 45 (2015).
8. Harris, E. V., de Roode, J. C. & Gerardo, N. M. Diet-microbiome-disease: investigating diet's influence on infectious disease resistance through alteration of the gut microbiome. *PLoS Pathog.* **15**, e1007891 (2019).
9. Wiertsema, S. P., van Bergenhenegouwen, J., Garssen, J. & Knippels, L. M. J. The interplay between the gut microbiome and the immune system in the context of infectious diseases throughout life and the role of nutrition in optimizing treatment strategies. *Nutrients* **13**, 886 (2021).
10. Imhann, F. et al. Proton pump inhibitors affect the gut microbiome. *Gut* **65**, 740–748 (2016).
11. Shon, A. S., Bajwa, R. P. & Russo, T. A. Hypervirulent (hypermucoviscous) Klebsiella pneumoniae: a new and dangerous breed. *Virulence* **4**, 107–118 (2013).
12. Paczosa, M. K. & Mecsas, J. Klebsiella pneumoniae: going on the offense with a strong defense. *Microbiol. Mol. Biol. Rev.* **80**, 629–661 (2016).
13. CDC. Healthcare-associated Infections. (Centers for Disease Control, 2018).
14. Khan, H. A., Baig, F. K. & Mehboob, R. Nosocomial infections: epidemiology, prevention, control and surveillance. *Asian. Pac. J.Trop. Bio.* **7**, 478–482 (2017).
15. Fung, C. P. et al. Klebsiella pneumoniae in gastrointestinal tract and pyogenic liver abscess. *Emerg. Infect. Dis.* **18**, 1322–1325 (2012).
16. Viau, R. A. et al. Silent" dissemination of Klebsiella pneumoniae isolates bearing K. pneumoniae carbapenemase in a long-term care facility for children and young adults in Northeast Ohio. *Clin. Infect. Dis.* **54**, 1314–1321 (2012).
17. Podschun, R. & Ullmann, U. Klebsiella spp. as nosocomial pathogens: epidemiology, taxonomy, typing methods, and pathogenicity factors. *Clin. Microbiol. Rev.* **11**, 589–603 (1998).
18. Russo, T. A. & Marr, C. M. Hypervirulent Klebsiella pneumoniae. *Clin. Microbiol. Rev.* **32**, e00001–00019 (2019).
19. Lin, Y. T. et al. Seroepidemiology of Klebsiella pneumoniae colonizing the intestinal tract of healthy Chinese and overseas Chinese adults in Asian countries. *BMC Microbiol.* **12**, 13 (2012).
20. Pollack, M. et al. Factors influencing colonisation and antibiotic-resistance patterns of gram-negative bacteria in hospital patients. *Lancet* **2**, 668–671 (1972).
21. Eberl, C. et al. E. coli enhance colonization resistance against Salmonella Typhimurium by competing for galactitol, a context-dependent limiting carbon source. *Cell Host Microbe* **29**, 1680–1692.e1687 (2021).
22. Nguyen, B. D. et al. Import of aspartate and malate by DcuABC Drives H(2)/fumarate respiration to promote initial salmonella gut-lumen colonization in mice. *Cell Host Microbe* **27**, 922–936.e926 (2020).
23. Litvak, Y. et al. Commensal Enterobacteriaceae protect against salmonella colonization through oxygen competition. *Cell Host Microbe* **25**, 128–139.e125 (2019).
24. Chassaing, B. & Cascales, E. Antibacterial weapons: targeted destruction in the microbiota. *Trends Microbiol.* **26**, 329–338 (2018).
25. Gillor, O., Giladi, I. & Riley, M. A. Persistence of colicinogenic Escherichia coli in the mouse gastrointestinal tract. *BMC Microbiol.* **9**, 165 (2009).
26. Portrait, V., Gendron-Gaillard, S., Cottenceau, G. & Pons, A. M. Inhibition of pathogenic Salmonella enteritidis growth mediated by Escherichia coli microcin J25 producing strains. *Canadian J. Microbiol.* **45**, 988–994 (1999).
27. Sassone-Corsi, M. et al. Microcins mediate competition among Enterobacteriaceae in the inflamed gut. *Nature* **540**, 280–283 (2016).
28. Young, T. M. et al. Animal model to study Klebsiella pneumoniae gastrointestinal colonization and host-to-host transmission. *Infect. Immun.* **88**, e00071–20 (2020).
29. Hudson, A. W., Barnes, A. J., Bray, A. S., Ornelles, D. A. & Zafar, M. A. *Klebsiella pneumoniae* l-Fucose metabolism promotes gastrointestinal colonization and modulates its virulence determinants. *Infect. Immun.* **90**, e0020622 (2022).
30. Bray, A. S. et al. MgrB-dependent colistin resistance in Klebsiella pneumoniae is associated with an increase in host-to-host transmission. *mBio* **13**, e03595–03521 (2022).
31. Sequeira, R. P., McDonald, J. A. K., Marchesi, J. R. & Clarke, T. B. Commensal Bacteroidetes protect against Klebsiella pneumoniae colonization and transmission through IL-36 signalling. *Nat. Microbiol.* **5**, 304–313 (2020).
32. Osbelt, L. et al. Klebsiella oxytoca causes colonization resistance against multidrug-resistant K. pneumoniae in the gut via cooperative carbohydrate competition. *Cell Host Microbe* **29**, 1663–1679.e1667 (2021).
33. Goodman, A. L. et al. Identifying genetic determinants needed to establish a human gut symbiont in its habitat. *Cell Host Microbe* **6**, 279–289 (2009).
34. Goodman, A. L., Wu, M. & Gordon, J. I. Identifying microbial fitness determinants by insertion sequencing using genome-wide transposon mutant libraries. *Nat. Protoc.* **6**, 1969–1980 (2011).
35. Agard, M. J., Ozer, E. A., Morris, A. R., Piseaux, R. & Hauser, A. R. A genomic approach to identify Klebsiella pneumoniae and Acinetobacter baumannii strains with enhanced competitive fitness in the lungs during multistrain pneumonia. *Infect. Immun.* **87**, e00871–00818 (2019).
36. Love, M. I., Huber, W. & Anders, S. Moderated estimation of fold change and dispersion for RNA-seq data with DESeq2. *Genome Biol.* **15**, 550 (2014).
37. Zhao, L., Anderson, M. T., Wu, W., Mobley, H. L. T & Bachman, M. A. TnseqDiff: identification of conditionally essential genes in transposon sequencing studies. *BMC Bioinformatics* **18**, 326 (2017).
38. Broberg, C. A., Wu, W., Cavalcoli, J. D., Miller, V. L. & Bachman, M. A. Complete genome sequence of Klebsiella pneumoniae strain ATCC 43816 KPPR1, a rifampin-resistant mutant commonly used in animal, genetic, and molecular biology studies. *Genome Announc.* **2**, e0094–14 (2014).
39. Ho, B. T., Dong, T. G. & Mekalanos, J. J. A view to a kill: the bacterial type VI secretion system. *Cell Host Microbe* **15**, 9–21 (2014).
40. Wu, K. M. et al. Genome sequencing and comparative analysis of Klebsiella pneumoniae NTUH-K2044, a strain causing liver abscess and meningitis. *J. Bacteriol.* **191**, 4492–4501 (2009).
41. Merciecca, T. et al. Role of Klebsiella pneumoniae Type VI secretion system (T6SS) in long-term gastrointestinal colonization. *Sci. Rep.* **12**, 16968 (2022).
42. Sarris, P. F., Zoumadakis, C., Panopoulos, N. J. & Scoulica, E. V. Distribution of the putative type VI secretion system core genes in Klebsiella spp. *Infect. Genet. Evol.* **11**, 157–166 (2011).
43. Wang, J. et al. Bastion6: a bioinformatics approach for accurate prediction of type VI secreted effectors. *Bioinformatics* **34**, 2546–2555 (2018).
44. Li, J. et al. SecReT6: a web-based resource for type VI secretion systems found in bacteria. *Environ. Microbiol.* **17**, 2196–2202 (2015).
45. Russell, A. B., Peterson, S. B. & Mougous, J. D. Type VI secretion system effectors: poisons with a purpose. *Nat. Rev. Microbiol.* **12**, 137–148 (2014).

46. Salomon, D. et al. Marker for type VI secretion system effectors. *Proc. Natl. Acad. Sci. USA.* **111**, 9271–9276 (2014).
47. Wang, J. et al. The conserved domain database in 2023. *Nucleic Acids Res.* **51**, D384–D388 (2023).
48. Hachani, A., Wood, T. E. & Filloux, A. Type VI secretion and anti-host effectors. *Curr. Opin. Microbiol.* **29**, 81–93 (2016).
49. Calderon-Gonzalez, R. et al. Modelling the gastrointestinal carriage of Klebsiella pneumoniae infections. *mBio* **14**, e0312122 (2023).
50. Xie, T., Rotstein, D., Sun, C., Fang, H. & Frucht, D. M. Gastric pH and toxin factors modulate infectivity and disease progression after gastrointestinal exposure to Bacillus anthracis. *J. Infect. Dis.* **216**, 1471–1475 (2017).
51. Woodward, S. E. et al. Gastric acid and escape to systemic circulation represent major bottlenecks to host infection by Citrobacter rodentium. *ISME J.* **17**, 36–46 (2023).
52. Cianfanelli, F. R., Monlezun, L. & Coulthurst, S. J. Aim, load, fire: the type VI secretion system, a bacterial nanoweapon. *Trends Microbiol.* **24**, 51–62 (2016).
53. Silverman, J. M., Brunet, Y. R., Cascales, E. & Mougous, J. D. Structure and regulation of the type VI secretion system. *Annu. Rev. Microbiol.* **66**, 453–472 (2012).
54. Lawlor, M. S., Hsu, J., Rick, P. D. & Miller, V. L. Identification of Klebsiella pneumoniae virulence determinants using an intranasal infection model. *Mol. Microbiol.* **58**, 1054–1073 (2005).
55. Wong Fok Lung, T. et al. Klebsiella pneumoniae induces host metabolic stress that promotes tolerance to pulmonary infection. *Cell Metab.* **34**, 761–774.e769 (2022).
56. Yi, X., Gao, J. & Wang, Z. The human lung microbiome—a hidden link between microbes and human health and diseases. *iMeta* **1**, e33 (2022).
57. Xu, N. et al. Microbiota dysbiosis in lung cancer: evidence of association and potential mechanisms. *Transl. Lung Cancer Res.* **9**, 1554–1568 (2020).
58. Castro-Mejía, J. L. et al. Gut microbiota recovery and immune response in ampicillin-treated mice. *Res. Vet. Sci.* **118**, 357–364 (2018).
59. Lawley, T. D. et al. Antibiotic treatment of clostridium difficile carrier mice triggers a supershedder state, spore-mediated transmission, and severe disease in immunocompromised hosts. *Infect. Immun.* **77**, 3661–3669 (2009).
60. Alteri, C. J. & Mobley, H. L. T. The versatile type VI secretion system. *Microbiol. Spectr.* **4**, vmbf-0026-2015 (2016).
61. Karp, P. D. et al. The EcoCyc database (2023). *EcoSal Plus* **11**, eesp00022023 (2023).
62. Lu, C. D. & Abdelal, A. T. Role of ArgR in activation of the ast operon, encoding enzymes of the arginine succinyltransferase pathway in Salmonella typhimurium. *J. Bacteriol.* **181**, 1934–1938 (1999).
63. Salmon, K. et al. Global gene expression profiling in Escherichia coli K12. The effects of oxygen availability and FNR. *J. Biol. Chem.* **278**, 29837–29855 (2003).
64. Gao, Y., Bang, I., Seif, Y., Kim, D. & Palsson, BernhardO. The Escherichia coli Fur pan-regulon has few conserved but many unique regulatory targets. *Nucleic Acids Res.* **51**, 3618–3630 (2023).
65. Cho, S. et al. The architecture of ArgR-DNA complexes at the genome-scale in *Escherichia coli*. *Nucleic Acids Res.* **43**, 3079–3088 (2015).
66. Myers, K. S. et al. Genome-scale analysis of Escherichia coli FNR reveals complex features of transcription factor binding. *PLoS Genet.* **9**, e1003565 (2013).
67. Chen, Z. et al. Discovery of Fur binding site clusters in Escherichia coli by information theory models. *Nucleic Acids Res.* **35**, 6762–6777 (2007).
68. Stojanov, S., Berlec, A. & Strukelj, B. The influence of probiotics on the Firmicutes/Bacteroidetes ratio in the treatment of obesity and inflammatory bowel disease. *Microorganisms* **8**, 1715 (2020).
69. DeGruttola, A. K., Low, D., Mizoguchi, A. & Mizoguchi, E. Current understanding of dysbiosis in disease in human and animal models. *Inflamm. Bowel Dis.* **22**, 1137–1150 (2016).
70. Cheng, A. G. et al. Design, construction, and in vivo augmentation of a complex gut microbiome. *Cell* **185**, 3617–3636.e3619 (2022).
71. Stewart, E. J. Growing unculturable bacteria. *J. Bacteriol.* **194**, 4151–4160 (2012).
72. Li, H. et al. Application of droplet digital PCR to detect the pathogens of infectious diseases. *Biosci. Rep.* **38**, BSR20181170 (2018).
73. Mougous, J. D., Gifford, C. A., Ramsdell, T. L. & Mekalanos, J. J. Threonine phosphorylation post-translationally regulates protein secretion in Pseudomonas aeruginosa. *Nature Cell Biol.* **9**, 797–803 (2007).
74. Russo, T. A. & Gill, S. R. Draft genome sequence of the hypervirulent Klebsiella pneumoniae strain hvKP1, isolated in Buffalo, New York. *Genome Announc* **1**, e0006513 (2013).
75. Le, N. H., V, Pinedo., J, Lopez., C, Cava., & M. F, Feldman. Killing of Gram-negative and Gram-positive bacteria by a bifunctional cell wall-targeting T6SS effector. *Proc. Natl. Acad. Sci. USA.* **118**, e2106555118 (2021).
76. Murray, C. J. L. et al. Global burden of bacterial antimicrobial resistance in 2019: a systematic analysis. *Lancet* **399**, 629–655 tabfig(2022).
77. Martin, R. M. et al. Molecular epidemiology of colonizing and infecting isolates of Klebsiella pneumoniae. *mSphere* **1**, e00261–16 (2016).
78. Raffelsberger, N. et al. Gastrointestinal carriage of Klebsiella pneumoniae in a general adult population: a cross-sectional study of risk factors and bacterial genomic diversity. *Gut Microbes* **13**, 1939599 (2021).
79. Bachman, M. A. et al. Genome-wide identification of Klebsiella pneumoniae fitness genes during lung infection. *mBio* **6**, e00775 (2015).
80. Jung, H. J. et al. Genome-wide screening for enteric colonization factors in Carbapenem-resistant ST258 Klebsiella pneumoniae. *mBio* **10**, e02663–18 (2019).
81. Cheung, B. H. et al. Genome-wide screens reveal shared and strain-specific genes that facilitate enteric colonization by Klebsiella pneumoniae. *mBio* **14**, e0212823 (2023).
82. Barnes, A. J. et al. Ethanolamine metabolism through two genetically distinct loci enables Klebsiella pneumoniae to bypass nutritional competition in the gut. *PLoS Pathog.* **20**, e1012189 (2024).
83. Chen, C., Yang, X. & Shen, X. Confirmed and potential roles of bacterial T6SSs in the intestinal ecosystem. *Front. Microbiol.* **10**, 1484 (2019).
84. Zhao, W., Caro, F., Robins, W. & Mekalanos, J. J. Antagonism toward the intestinal microbiota and its effect on Vibrio cholerae virulence. *Science* **359**, 210–213 (2018).
85. Wan, B. et al. Type VI secretion system contributes to Enterohemorrhagic Escherichia coli virulence by secreting catalase against host reactive oxygen species (ROS). *PLoS Pathog.* **13**, e1006246 (2017).
86. Anderson, M. C., Vonaesch, P., Saffarian, A., Marteyn, B. S. & Sansonetti, P. J. Shigella sonnei encodes a functional T6SS used for interbacterial competition and niche occupancy. *Cell Host Microbe* **21**, 769–776.e3 (2017).
87. Sana, T. G. et al. Salmonella Typhimurium utilizes a T6SS-mediated antibacterial weapon to establish in the host gut. *Proc. Natl. Acad. Sci. USA.* **113**, E5044–5051 (2016).
88. Coulthurst, S. The Type VI secretion system: a versatile bacterial weapon. *Microbiology* **165**, 503–515 (2019).

89. Serapio-Palacios, A. et al. Type VI secretion systems of pathogenic and commensal bacteria mediate niche occupancy in the gut. *Cell Rep.* **39**, 110731 (2022).
90. Osbelt, L. et al. Variations in microbiota composition of laboratory mice influence Citrobacter rodentium infection via variable short-chain fatty acid production. *PLoS Pathog.* **16**, e1008448 (2020).
91. Bernard, C. S., Brunet, Y. R., Gueguen, E. & Cascales, E. Nooks and crannies in type VI secretion regulation. *J. Bacteriol.* **192**, 3850–3860 (2010).
92. Miyata, S. T., Bachmann, V. & Pukatzki, S. Type VI secretion system regulation as a consequence of evolutionary pressure. *J. Med. Microbiol.* **62**, 663–676 (2013).
93. Chen, L., Zou, Y., She, P. & Wu, Y. Composition, function, and regulation of T6SS in Pseudomonas aeruginosa. *Microbiol. Res.* **172**, 19–25 (2015).
94. Barbosa, V. A. A. & Lery, L. M. S. Insights into Klebsiella pneumoniae type VI secretion system transcriptional regulation. *BMC Genomics* **20**, 506 (2019).
95. Storey, D. et al. Klebsiella pneumoniae type VI secretion system-mediated microbial competition is PhoPQ controlled and reactive oxygen species dependent. *PLoS Pathog.* **16**, e1007969 (2020).
96. Adibi, S. A. & Mercer, D. W. Protein digestion in human intestine as reflected in luminal, mucosal, and plasma amino acid concentrations after meals. *J. Clin. Investig.* **52**, 1586–1594 (1973).
97. Friedman, E. S. et al. Microbes vs. chemistry in the origin of the anaerobic gut lumen. *Proc. Natl. Acad. Sci. USA.* **115**, 4170–4175 (2018).
98. Yilmaz, B. & Li, H. Gut microbiota and iron: the crucial actors in health and disease. *Pharmaceuticals* **11**, 98 (2018).
99. Wang, S. et al. The ferric uptake regulator represses type VI secretion system function by binding directly to the clpV promoter in Salmonella enterica Serovar Typhimurium. *Infect. Immun.* **87**, e00562–19 (2019).
100. Brunet, Y. R., Bernard, C. S., Gavioli, M., Lloubes, R. & Cascales, E. An epigenetic switch involving overlapping fur and DNA methylation optimizes expression of a type VI secretion gene cluster. *PLoS Genet.* **7**, e1002205 (2011).
101. Chakraborty, S., Sivaraman, J., Leung, K. Y. & Mok, Y. K. Two-component PhoB-PhoR regulatory system and ferric uptake regulator sense phosphate and iron to control virulence genes in type III and VI secretion systems of Edwardsiella tarda. *J. Biol. Chem.* **286**, 39417–39430 (2011).
102. Barbieri, N. L. et al. FNR regulates the expression of important virulence factors contributing to the pathogenicity of avian pathogenic Escherichia coli. *Front. Cell. Infect. Microbiol.* **7**, 265 (2017).
103. Bernard, C. S., Brunet, Y. R., Gavioli, M., Lloubès, R. & Cascales, E. Regulation of type VI secretion gene clusters by sigma54 and cognate enhancer binding proteins. *J. Bacteriol.* **193**, 2158–2167 (2011).
104. Zafar, M. A., Carabetta, V. J., Mandel, M. J. & Silhavy, T. J. Transcriptional occlusion caused by overlapping promoters. *Proc. Natl. Acad. Sci. USA.* **111**, 1557–1561 (2014).
105. Henson, M. A. & Phalak, P. Microbiota dysbiosis in inflammatory bowel diseases: in silico investigation of the oxygen hypothesis. *BMC Syst. Biol.* **11**, 145 (2017).
106. Zhu, H. & Li, Y. R. Oxidative stress and redox signaling mechanisms of inflammatory bowel disease: updated experimental and clinical evidence. *Exp. Biol. and Med.* **237**, 474–480 (2012).
107. Bachmann, V. et al. Bile salts modulate the mucin-activated type VI secretion system of pandemic Vibrio cholerae. *PLoS Negl. Trop. Dis.* **9**, e0004031 (2015).
108. Martin, R. M. & Bachman, M. A. Colonization, infection, and the accessory genome of Klebsiella pneumoniae. *Front. Cell. Infect. Microbiol.* **8**, 4 (2018).
109. Krych, L., Hansen, C. H., Hansen, A. K., van den Berg, F. W. & Nielsen, D. S. Quantitatively different, yet qualitatively alike: a meta-analysis of the mouse core gut microbiome with a view towards the human gut microbiome. *PloS One* **8**, e62578 (2013).
110. US Department of Health and Human Services. *Public Health Service policy on humane care and use of laboratory animals*. (2015).
111. Worlein, J. M., Baker, K., Bloomsmith, M., Coleman, K. & Koban, T. L. *The Eighth Edition of the Guide for the Care and Use of Laboratory Animals (2011); Implications for Behavioral Management*. Vol. 73 (2011).
112. Datsenko, K. A. & Wanner, B. L. One-step inactivation of chromosomal genes in Escherichia coli K-12 using PCR products. *Proc. Natl. Acad. Sci. USA.* **97**, 6640–6645 (2000).
113. Skorupski, Karen R. K. T. Positive selection vectors for allelic exchange. *Gene* **169**, 47-52 (1995).
114. Ramage, B. et al. Comprehensive arrayed transposon mutant library of Klebsiella pneumoniae outbreak strain KPNIH1. *J. Bacteriol.* **199**, e00352–17 (2017).
115. Palacios, M., Broberg, C. A., Walker, K. A. & Miller, V. L. A serendipitous mutation reveals the severe virulence defect of a Klebsiella pneumoniae fepB mutant. *mSphere* **2**, e00341–00317 (2017).
116. Choi, K.-H. et al. A Tn7-based broad-range bacterial cloning and expression system. *Nat. Methods* **2**, 443–448 (2005).
117. Miller, W. G., Leveau, J. H. & Lindow, S. E. Improved gfp and inaZ broad-host-range promoter-probe vectors. *Mol. Plant Microbe Interact.* **13**, 1243–1250 (2000).
118. Walker, K. A. et al. A Klebsiella pneumoniae regulatory mutant has reduced capsule expression but retains hypermucoviscosity. *mBio* **10**, e00089–00019 (2019).
119. Lazazzera, B. A., Bates, D. M. & Kiley, P. J. The activity of the Escherichia coli transcription factor FNR is regulated by a change in oligomeric state. *Gene Dev.* **7**, 1993–2005 (1993).
120. Palacios, M. et al. Identification of two regulators of virulence that are conserved in Klebsiella pneumoniae classical and hypervirulent strains. *mBio* **9**, e01443–01418 (2018).
121. Zoetendal, E. G. et al. Isolation of RNA from bacterial samples of the human gastrointestinal tract. *Nat. Protoc.* **1**, 954–959 (2006).
122. Livak, K. J. & Schmittgen, T. D. Analysis of relative gene expression data using real-time quantitative PCR and the $2^{-\Delta\Delta CT}$ method. *Methods* **25**, 402–408 (2001).
123. Zafar, M. A. et al. Identification of pneumococcal factors affecting pneumococcal shedding shows that the dlt locus promotes inflammation and transmission. *mBio* **10**, e01032–01019 (2019).
124. Ziegelhoffer, E. C. & Kiley, P. J. In vitro analysis of a constitutively active mutant form of the Escherichia coli global transcription factor FNR. *J. Mol. Biol.* **245**, 351–361 (1995).
125. Brand, L. H., Kirchler, T., Hummel, S., Chaban, C. & Wanke, D. DPI-ELISA: a fast and versatile method to specify the binding of plant transcription factors to DNA in vitro. *Plant Methods* **6**, 25 (2010).
126. Ottesen, A. et al. Enrichment dynamics of Listeria monocytogenes and the associated microbiome from naturally contaminated ice cream linked to a listeriosis outbreak. *BMC Microbiol.* **16**, 275 (2016).
127. Ponnusamy, D. et al. Cross-talk among flesh-eating strains in mixed infection leading to necrotizing fasciitis. *Proc. Natl. Acad. Sci. USA.* **113**, 722–727 (2016).
128. Hasan, N. A. et al. Microbial community profiling of human saliva using shotgun metagenomic sequencing. *PloS One* **9**, e97699 (2014).
129. Lax, S. et al. Longitudinal analysis of microbial interaction between humans and the indoor environment. *Science* **345**, 1048–1052 (2014).
130. Lahti, L. & Shetty, S. *Tools for microbiome analysis in R. Microbiome package version 1.23.1*, http://microbiome.github.io/microbiome (2017).

131. McMurdie, P. J. & Holmes, S. phyloseq: an R package for reproducible interactive analysis and graphics of microbiome census data. *PloS One* **8**, e61217 (2013).
132. Pinheiro, L. B. et al. Evaluation of a droplet digital polymerase chain reaction format for DNA copy number quantification. *Anal. Chem.* **84**, 1003–1011 (2012).
133. Boudeau, J., Barnich, N. & Darfeuille-Michaud, A. Type 1 pili-mediated adherence of Escherichia coli strain LF82 isolated from Crohn's disease is involved in bacterial invasion of intestinal epithelial cells. *Mol. Microbiol.* **39**, 1272–1284 (2001).
134. Chenault, S. S. & Earhart, C. F. Identification of hydrophobic proteins FepD and FepG of the Escherichia coli ferrienterobactin permease. *J. Gen. Microbiol.* **138**, 2167–2171 (1992).
135. Fetherston, J. D., Bertolino, V. J. & Perry, R. D. YbtP and YbtQ: two ABC transporters required for iron uptake in Yersinia pestis. *Mol. Microbiol.* **32**, 289–299 (1999).
136. Sgro, G. G. et al. Bacteria-killing type IV secretion systems. *Front. Microbiol.* **10**, 1078 (2019).
137. Chivers, P. T., Benanti, E. L., Heil-Chapdelaine, V., Iwig, J. S. & Rowe, J. L. Identification of Ni-(L-His)$_2$ as a substrate for NikABCDE-dependent nickel uptake in Escherichia coli. *Metallomics* **4**, 1043–1050 (2012).
138. Daley, D. O. et al. Global topology analysis of the Escherichia coli inner membrane proteome. *Science* **308**, 1321–1323 (2005).
139. Clementz, T., Bednarski, J. J. & Raetz, C. R. Function of the htrB high temperature requirement gene of Escherichia coli in the acylation of lipid A: HtrB catalyzed incorporation of laurate. *J. Biol. Chem.* **271**, 12095–12102 (1996).
140. Breazeale, S. D., Ribeiro, A. A. & Raetz, C. R. Origin of lipid A species modified with 4-amino-4-deoxy-L-arabinose in polymyxin-resistant mutants of Escherichia coli. An aminotransferase (ArnB) that generates UDP-4-deoxyl-L-arabinose. *J. Biol. Chem.* **278**, 24731–24739 (2003).
141. Eckford, P. D. & Sharom, F. J. The reconstituted Escherichia coli MsbA protein displays lipid flippase activity. *Biochem. J.* **429**, 195–203 (2010).
142. Uehara, T., Parzych, K. R., Dinh, T. & Bernhardt, T. G. Daughter cell separation is controlled by cytokinetic ring-activated cell wall hydrolysis. *EMBO J.* **29**, 1412–1422 (2010).
143. Terui, Y. et al. Properties of putrescine uptake by PotFGHI and PuuP and their physiological significance in Escherichia coli. *Amino Acids* **46**, 661–670 (2014).
144. Thöny-Meyer, L., Fischer, F., Künzler, P., Ritz, D. & Hennecke, H. Escherichia coli genes required for cytochrome c maturation. *J. Bacteriol.* **177**, 4321–4326 (1995).
145. Jin, F. et al. The structure of MgtE in the absence of magnesium provides new insights into channel gating. *PLoS Biol.* **19**, e3001231 (2021).
146. Rahn, A. & Whitfield, C. Transcriptional organization and regulation of the Escherichia coli K30 group 1 capsule biosynthesis (cps) gene cluster. *Mol. Microbiol.* **47**, 1045–1060 (2003).

Acknowledgements

We are grateful for the members of the Zafar and Miller laboratories for fruitful discussions and comments on the manuscript. This project was supported by AI178595, AI166642, and AI173244 from NIAID to M.A.Z. as well as start-up funds from Wake Forest School of Medicine. Additional support came from AI132925 (NIAID) to V.L.M. A.S.B. was supported by 5T32AI007401 from NIAID and T32GM127261 from NIGMS. C.A.B. was supported by T32AI007151 from NIAID. G.E.H. was supported by T32AI007401, AI173244 diversity supplement award from NIAID, and through the Burroughs Wellcome Fund graduate diversity enrichment program. A.J.B. and A.W.H. were supported by the graduate program funds provided by the Wake Forest School of Medicine. The funders had no role in study design, data collection and analysis, decision to publish, or preparation of the manuscript.

Author contributions

M.A.Z. designed and acquired funding for the study; A.S.B. and T.M.Y. performed the Tn-seq, and W.W. carried out the analysis; R.K.N. and A.S.B. processed and analyzed microbiome data; C.A.B. and A.S.B. constructed knockout strains used in the study; A.S.B. constructed plasmids used in the study; A.S.B., C.A.B., G.E.H., E.F.B. and A.J.B. performed the murine infection studies; A.S.B., A.W.H., M.M.I., J.D.V., F.S. and A.J.B. performed molecular assays described in the study. A.S.B., R.K.N., N.A.N., K.A.W., D.A.O., V.L.M. and M.A.Z. helped with data analysis; A.S.B. wrote the manuscript, and K.A.W., V.L.M. and M.A.Z. edited the manuscript.

Competing interests

The authors declare no competing interests.

Additional information

Supplementary information The online version contains supplementary material available at https://doi.org/10.1038/s41467-025-56309-8.

Correspondence and requests for materials should be addressed to M. Ammar Zafar.

Peer review information *Nature Communications* thanks Jin-Town Wang, and the other, anonymous, reviewer(s) for their contribution to the peer review of this work. A peer review file is available.